Deliverable D-7
TN-5: Booklet with Numerical Ablation Test Cases

Relating and contributing to WP5:
Definition of Numerical Test Cases (Booklet)

28 September, 2018

Author(s):	F. Pascon	
	T. van Eekelen	
	L. Chipperfield	
	A. Turchi	
Checked:	A. Turchi	
Approved:	T. Magin	
Authorized:	O. Chazot	

Contents

Applicable documents

[AD1] Ablative TPS numerical test cases mathematical code assessment & improvement. Appendix 1 to AO/1-9091/17/NL/RA, issue 1 rev. 3. Prepared by ESA ESTEC, 2017.

[AD2] Ablative TPS numerical test cases mathematical code assessment & improvement: Technical, Implementation, Management and Financial Proposal. Prepared by the AblaNTIS consortium in response to ESA AO/1-9091/17/NL/RA, 2017.

[AD3] AblaNTIS: Negotiation meeting minutes and attachments. ref: AblaNTIS_MoM_1, December 2017.

[AD4] AblaNTIS: Kickoff meeting minutes and attachments. ref: AblaNTIS_MoM_2, February 2018.

[AD5] AblaNTIS Deliverable D-1 TN-1: Detailed Work Plan. ref: AblaNTIS_D-1_TN-1, May 2018.

Reference documents

[RD1] Jean Lachaud, Alexandre Martin, Ioana Cozmuta, and Bernie Laub. Ablation test case 1. In *4th Ablation Workshop*.

[RD2] Jean Lachaud, Alexandre Martin, Tom van Eekelen, and Ioana Cozmuta. Ablation test case 2. In *5th Ablation Workshop*.

[RD3] Jean Lachaud, Alexandre Martin, Tom van Eekelen, and Ioana Cozmuta. Ablation test case 3. In *5th Ablation Workshop*.

[RD4] AblaRadAbla: Plasmatron test preparation and execution. ESA Contract 40001131101/15/NL/RA, ref: TR2v2, prepared by von Karman Institute for Fluid Dynamics, November 2017.

[RD5] Mersen. Properties of CALCARB rigid carbon insulation CBCF 18-2000. Manufacturer datasheet.

[RD6] ZURAM® material data–v2.0.0. Excel Spreadsheet prepared by the German Aerospace Center, April 2018.

[RD7] TACOT_v3.0.xlsx – Properties of the Theoretical Ablative Composite for Open Testing (TACOT). Excel Spreadsheet prepared for 6th US Ablation Workshop.

[RD8] F. J. Torres Herrador. Thermal Characterization of Ablative Materials. Technical report, von Karman Institute for Fluid Dynamics, 2018.

[RD9] F. J. Torres Herrador. Experimental characterization and simulation of pyrolysis phenomenon: from carbon composite ablators to Pacific Islands plant biomass. Technical report, von Karman Institute for Fluid Dynamics, 2017. VKI PR 2017-23.

[RD10] MA Covington, JM Heinemann, HE Goldstein, Y-K Chen, I Terrazas-Salinas, JA Balboni, J Olejniczak, and ER Martinez. Performance of a low density ablative heat shield material. *Journal of Spacecraft and Rockets*, 45(2):237–247, 2008.

[RD11] G Chambre P Reynier. ISA TN-04-2007 – Test case definition for numerical rebuilding within the european ablation working group. October 2007.

1. Introduction

The main objective of Task 5 is the definition of ablation numerical test cases and the edition of a booklet (this document) with detailed descriptions of these test cases for distribution to the community.

In the Detailed Work Plan document (Deliverable 1 – TN-1 [AD5]), a set of 17 numerical test cases have been drawn up, based on:

1. already available data, i.e.
   - the ablation test-case series 1, 2 and 3 of the 4^{th} and 5^{th} Ablation Workshops [RD1, RD2, RD3]
   - the AblaRadAbla Plasmatron tests results [RD4]
2. the preliminary definition of the experimental tests to be performed (cf. Task 3 – Plasma Testing) and the foreseen results

These numerical tests and their naming convention are listed in section 2 of this document.

Two different materials[1] are considered in the numerical test cases: CALCARB® and ZURAM®. The material properties required for running the thermal-response codes selected in this project have been identified and a list of "common" input parameters and properties for both materials in the various states (i.e., virgin, char, pyrolysis gas) are detailed in section 3.

Two types of test cases are planned:

1. one-dimensional planar test cases — these tests are purely numerical (there will be no experimental validation) and are intended for code-to-code comparison only;
2. two-dimensional hemispherical test cases — these tests will be compared with the results of Plasmatron runs.

The geometry and the boundary conditions related to these two types of tests are detailed in section 4.

The output results as well as the file format (selected to ease code-to-code comparison) are defined in section 5.

The final section is dedicated to the detailed description of each numerical test case, including:

[1] Test cases with CALCARB® are designed to allow a step-by-step evolution in the tests complexity, the preform being not subjected to pyrolysis.

- the test-case description,
- the corresponding assumptions and simplifications,
- the material properties to be used (referring to the values introduced in section 3),
- the boundary conditions (referring to the values introduced in section 4),
- the requested output results.

Remark:

The present document will be evolving along the project:

1. Issue 1 is
   - a collection of initial available data, i.e. the available experimental properties for ZURAM® and some dummy values (from similar materials or from TACOT) where data is limited or missing [AD5]
   - a definition of the test cases that will be rebuilt to see if the models works as expected
2. Issue 2 contains the implementation of
   - the material characterization (WP2)
   - the plasma tests results (WP3)
3. Issue 3 (final issue) is including numerical tests results, conclusions and recommendations.

2. Naming convention of the numerical test cases

As introduced in the Detailed Work Plan document (Deliverable 1 – TN-1 [AD5]), all the test cases (listed in Table 1) follow the naming convention

[Num/Exp]-N-[T/SEB]-[P/Z]

where:

- **Num/Exp**:
  - **Num**, the test case involves code-to-code comparison only. These tests are identical to the US Ablation Workshop test cases with the exception that the ZURAM® material properties are used instead of the "fictitious" material TACOT. Therefore, these tests do not depend in any way on the plasma tests performed within Task 3.
  - **Exp**, the test case includes comparison with tests performed in the Plasmatron. Some of these tests are repetitions of to the tests already performed in AblaRadAbla (cf. Table 3).
- **N**: test case condition number, i.e. one value per combination of heat flux and atmosphere (N_2 or air).
- **T/SEB**:
  - **T**, the surface boundary temperature, pressure and recession rate are predefined functions of time and surface location.
  - **SEB**, the surface boundary conditions are found by satisfying the surface energy balance (SEB), with a convective heat flux that is a function of time and surface location.
- **P/Z**:
  - **P**, the sample material will be CALCARB® .
  - **Z**, the sample material will be ZURAM® .

Together with this short list, the conditions (physical phenomena) that will be active in each of the test cases are summarized in Table 2.

An extended description of each numerical test case can be found in section 6 of this document.

Table 1: List of numerical test cases

Numer. test ID	Plasm. exper. ID (or code-to-code)	Geometry	Material	Heat flux ⋆ [MW/m^2]	Gas	B.C.	Duration [s]	max T_w † [K]	P_w [hPa]
Num-1-T-P	code-to-code	1D, planar	CALCARB®	n.a.	n.a.	T_w	120	1500	50
Num-1-T-Z	code-to-code	1D, planar	ZURAM®	n.a.	n.a.	T_w	120	1500	50
Num-2-SEB-Z	code-to-code	1D, planar	ZURAM®	0.5	Air	SEB	120	n.a.	50
Num-3-SEB-Z	code-to-code	1D, planar	ZURAM®	1.5	Air	SEB	120	n.a.	50
Num-4-SEB-Z	code-to-code	1D, planar	ZURAM®	5.0	Air	SEB	120	n.a.	50
Exp-1-T-P	P-N-50-q300	2D, hemisphere	CALCARB®	0.3	N_2	T_w,$\dot{r}$	120	n.a.	50
Exp-1-SEB-P	P-N-50-q300	2D, hemisphere	CALCARB®	0.3	N_2	SEB	120	n.a.	50
Exp-2-T-Z	Z-A-50-q300	2D, hemisphere	ZURAM®	0.3	Air	T_w,$\dot{r}$	120	n.a.	50
Exp-2-SEB-Z	Z-A-50-q300	2D, hemisphere	ZURAM®	0.3	Air	SEB	120	n.a.	50
Exp-3-T-P	P-N-100-q2500	2D, hemisphere	CALCARB®	2.5	N_2	T_w,$\dot{r}$	34	n.a.	100
Exp-3-SEB-P	P-N-100-q2500	2D, hemisphere	CALCARB®	2.5	N_2	SEB	34	n.a.	100
Exp-3-T-Z	Z-N-100-q2500	2D, hemisphere	ZURAM®	2.5	N_2	T_w,$\dot{r}$	30	n.a.	100
Exp-3-SEB-Z	Z-N-100-q2500	2D, hemisphere	ZURAM®	2.5	N_2	SEB	30	n.a.	100
Exp-4-T-Z	Z-A-100-q2500	2D, hemisphere	ZURAM®	2.5	Air	T_w,$\dot{r}$	30	n.a.	100
Exp-4-SEB-Z	Z-A-100-q2500	2D, hemisphere	ZURAM®	2.5	Air	SEB	30	n.a.	100
Exp-5-T-Z	SS-Z-A	2D, hemisphere	ZURAM®	4.5	Air	T_w,$\dot{r}$ ‡	TBD	n.a.	TBD
Exp-5-SEB-Z	SS-Z-A	2D, hemisphere	ZURAM®	4.5	Air	SEB	TBD	n.a.	TBD

⋆ Cold-wall heat flux

† The maximum wall temperature T_w is set to 1500K for the tests Num-1-T-P and Num-1-T-Z. For all the other tests, it is a priori unknown and it will be later defined for prescribed-temperature 2D tests (Exp-i-T-j), when experimental test measurements will be available.

‡ The recession and the surface temperature may be inaccurately measured.

Table 2: Physical phenomena that are included in the tests

Test ID	2D effects	λ_c	λ_v	Pyrolysis	Convective heat transfer	Oxid.	Subl.	Recession	Shape change	Non-equil.rad. (Potential†)
Num-1-T-P	-	✓	-	-	-	-	-	-	-	-
Num-1-T-Z	-	✓	✓	✓	✓	-	-	-	-	-
Num-2-SEB-Z	-	✓	✓	✓	✓	✓	-	-	-	-
Num-3-SEB-Z	-	✓	✓	✓	✓	✓	-	✓	-	-
Num-4-SEB-Z	-	✓	✓	✓	✓	✓	✓	✓	-	-
Exp-1-T-P	✓	✓	-	-	-	-	-	-	-	-
Exp-1-SEB-P	✓	✓	-	-	-	-	-	-	-	-
Exp-2-T-Z	✓	✓	✓	✓	✓	✓	-	-	-	-
Exp-2-SEB-Z	✓	✓	✓	✓	✓	✓	-	-	-	-
Exp-3-T-P	✓	✓	-	-	-	-	-	✓	-	✓
Exp-3-SEB-P	✓	✓	-	-	-	-	-	✓	-	✓
Exp-3-T-Z	✓	✓	✓	✓	✓	-	-	✓	-	-
Exp-3-SEB-Z	✓	✓	✓	✓	✓	-	-	✓	-	-
Exp-4-T-Z	✓	✓	✓	✓	✓	✓	-	✓	-	-
Exp-4-SEB-Z	✓	✓	✓	✓	✓	✓	-	✓	-	-
Exp-5-T-Z	✓	✓	✓	✓	✓	✓	✓	✓	✓	✓
Exp-5-SEB-Z	✓	✓	✓	✓	✓	✓	✓	✓	✓	✓

† The introduction of non-equilibrium radiation in the numerical models is limited to the re-run of tests EXP-3-j-P and EXP-5-j-Z after Plasmatron and characterization tests execution, as mentioned in the Detailed Work Plan document D-1 TN-1 [AD5]

Table 3: List of Plasmatron ablation experiments to be performed. "No. of tests" indicates the total amount of identical tests to be performed; "Repeated" indicates if the test is a repetition of a test performed (either in previous or in the present test campaign); "AbraRad. ref." indicates to which test of the AblaRadAbla TRP [RD4] the present test is linked.

Material	Shape	Flow	Gas	Cold-wall heat flux [MW/m^2]	No. of tests	Repeated	AblaRad. ref.
CALCARB®	Hemisph.	SUB	N_2	0.3	1	No	ZU1
CALCARB®	Hemisph.	SUB	N_2	2.5	1	No	ZU2
ZURAM®	Hemisph.	SUB	Air	0.3	1	Yes	ZU1
ZURAM®	Hemisph.	SUB	N_2	2.5	1	Yes	ZU4
ZURAM®	Hemisph.	SUB	Air	2.5	1	Yes	ZU2
ZURAM®	Hemisph.	SUP	Air	4.6	2	Yes (2 tests)	-

3. Material properties

In all the numerical test cases the samples will composed of either CALCARB® CBCF 18-2000 , or ZURAM® 18/50 material.

CALCARB® is a carbon fibre preform that can be impregnated with a phenolic resin to prepare ZURAM®. As CALCARB® does not pyrolyse, fewer material properties are required to characterize its behavior.

For ZURAM® (the reference material of the present activity), the list of "common" input parameters and properties set in the Detailed Work Plan document (Deliverable 1 – TN-1 [AD5]) are given in the Table 4.

Table 4: List of necessary input parameters/properties for the thermal-response simulation of charring ablators. The "-" indicates non-applicable quantities, e.g., pyrolysis rate of the material in charred state.

	Property	ZURAM® virgin	ZURAM® char	CALCARB®
Composition	Open porosity	✓	✓	✓
	Volume fractions	✓	✓	✓
	Intrinsic densities	✓	✓	✓
	Elemental composition	✓	✓	-
Chemistry	Overall pyrolysis rate	✓	-	-
Transport	Permeability	✓	✓	✓
	Tortuosity†	✓	✓	✓
Energy	Heat capacity	✓	✓	✓
	Formation enthalpy	✓	✓	-
	Effective conductivity	✓	✓	✓
	Heat of pyrolysis	✓	-	-
	Emissivity	✓	✓	✓

† Tortuosity is not foreseen to be used in any of the codes selected for computing the numerical test cases of this project, but it is given as an indicative value.

3.1. CALCARB® material properties

3.1.1. Open porosity

The open porosity in CALCARB® is 89 % [RD5].

3.1.2. Volume fractions

The volume fraction is 0.11 for fibers, and 0.89 for gas [RD5].

3.1.3. Intrinsic densities

The bulk density of CALCARB® is 180 kg/m^3 [RD5]. Combined with the porosity of 89 %, the intrinsic density of the fibers is, therefore, 1636.4 kg/m^3.

3.1.4. Permeability

The permeability of CALCARB® is 5.952 10^{-13} m^2 [RD6].

3.1.5. Tortuosity

The tortuosity[2] of CALCARB® is 1.1 [RD7].

3.1.6. Heat capacity

Based on the Reference [RD8], the heat capacity c_p [J/(kg.K)] of CALCARB® is given as a table (function of the temperature T [K]) in the `Tacot_Zuram_Calcarb_database.ods` data file (cf. Appendix B).

3.1.7. Effective conductivity

The thermal conductivity, k [W/(m.K)], of CALCARB® is defined by two functions: one along the through-the-thickness direction (k_{zz}), and one along the in-plane directions ($k_{xx} = k_{yy}$).

Both functions are available as tables of values (function of the temperature T [K]) in the `Tacot_Zuram_Calcarb_database.ods` data file (cf. Appendix 6.4).

3.1.8. Emissivity

The emissivity of CALCARB® is 0.90 [RD7]

[2] not used in any of the selected codes, but given as an indicative value

3.2. ZURAM® material properties

Note: Some of the following preliminary values of ZURAM® properties (labelled with a U) are estimated and will be later updated according to the results of the material characterization activity, WP-2.2

3.2.1. Open porosity

The open porosity of ZURAM® is U 55.58 % in the virgin state and U 70.76 % in the charred state [RD6]. The intermediate values (charring ZURAM®) is based on the density:

$$\varepsilon = \frac{\rho_\mathrm{v}\varepsilon_\mathrm{v} - \dfrac{\rho_\mathrm{v}-\rho}{\rho_\mathrm{v}-\rho_\mathrm{c}}\left(\rho_\mathrm{v}\varepsilon_\mathrm{v} - \rho_\mathrm{c}\varepsilon_\mathrm{c}\right)}{\rho} \tag{1}$$

3.2.2. Volume fractions

The volume fractions are [RD6, RD9]:

- virgin ZURAM® : 0.11 for fibers, U 0.3342 for resin, and U 0.5558 for gas
- charred ZURAM® : 0.11 for fibers, U 0.1824 for resin, and U 0.7076 for gas

3.2.3. Intrinsic densities

The bulk densities are [RD6]: 430 kg/m^3 for virgin ZURAM® and U 344 kg/m^3 for charred ZURAM® ; fibers (CALCARB®) have a bulk density of 180 kg/m^3 (assumed to be the same in the virgin and the charred states). The bulk density of the resin is therefore obtained by subtracting fibers from the composite, i.e. 250 kg/m^3 for virgin resin and U 164 kg/m^3 for charred resin.

Considering the volume fractions of fibers and resin (section 3.2.2), the intrinsic densities are therefore:

- fibers: $\dfrac{180}{0.11} = 1636.4$ kg/m^3
- virgin resin matrix: U $\dfrac{250}{0.3342} = 748.1$ kg/m^3
- charred resin matrix: U $\dfrac{164}{0.5558} = 899.1$ kg/m^3

3.2.4. Elemental composition of pyrolysis gas

The average elemental composition of the pyrolysis gases is obtained from TGA data by VKI on ZURAM® 18-50 [RD9]:

Element	mole fraction	mass fraction	molar mass [g/mol]
C	0.1245621	0.352	12.0107
H	0.7505798	0.178	1.00794
O	0.1248581	0.470	15.999
Total	1	1	4.250

Table 5: Average elemental composition of the pyrolysis gases for ZURAM®

The details are available in the document `Tacot_Zuram_Calcarb_database.ods` (see Appendix C). This data should not be updated but will be verified through the planned TGA test campaign. An update will be performed in case of discrepancies.

3.2.5. Overall pyrolysis rate

Two pseudo-phases are considered: inert fibers and resin that is decomposing to char. The resin pyrolysis kinetics is characterized by three Arrhenius-type equations and corresponding density loss fractions F_i, such that the pyrolysis gas generation rate, Π, is given by Equation 2 and the rate of change in the extent of reaction, ξ_j, of component j is given by Equation 3.

$$\Pi = -\frac{\partial \left(\varepsilon_m \, \rho_m\right)}{\partial t} = \varepsilon_{m,v} \, \rho_{m,v} \sum_{i=1}^{3} F_i \frac{\partial \xi_i}{\partial t} \tag{2}$$

$$\frac{\partial \xi_i}{\partial t} = \left(1 - \xi_i\right)^{n_i} A_i \exp \frac{-E_i}{RT} \tag{3}$$

where the index v denotes the virgin state (unpyrolysed material), ε_m is the resin volume fraction and ρ_m is the intrinsic density of the resin phase.

The constants in the three Arrhenius rate equations are given in Table 6 [RD9].

reaction	F_i	A_i [s^{-1}]	E_i/R [K]	n_i
1	0.035	66671	8576.7	5
2	0.029	825593	13302.3	2.9
3	0.147	9499	11951.9	2.2

Table 6: Pyrolysis kinetics for ZURAM®

This data should not be updated but will be verified through the planned TGA test campaign. An update will be performed in case of discrepancies.

3.2.6. Permeability

The permeability is U $2.312\,10^{-13}$ m^2 for virgin ZURAM® , and U $5.952\,10^{-13}$ m^2 for charred ZURAM® [RD6].

3.2.7. Tortuosity

The tortuosity[3] is 1.2 for virgin ZURAM® and 1.1 for charred ZURAM® [RD7].

3.2.8. Heat capacity

The heat capacity c_p [J/(kg.K)] of ZURAM® is given as tables (function of the temperature T [K]) in the `Tacot_Zuram_Calcarb_database.ods` data file (cf. Appendix C). There are two different definitions:

1. for decomposing[4] ZURAM®
2. for charred ZURAM®

3.2.9. Formation enthalpy

The formation enthalpy of char at 298 K is set as the reference (zero), so that it is equal to -2 10^6 J/kg for pure phenolic resin, and -1.163 10^6 J/kg for virgin ZURAM® [RD10].

3.2.10. Effective conductivity U

For each state (decomposing and charred), the thermal conductivity k [W/(m.K)] of ZURAM® is defined by two functions: one along the through-the-thickness direction (k_{zz}), and one along the in-plane directions ($k_{xx} = k_{yy}$).

All the functions are available as tables of values (function of the temperature T [K]) in the `Tacot_Zuram_Calcarb_database.ods` data file (cf. Appendix C).

[3] not used in any of the selected codes, but given as an indicative value

[4] based on the heat capacity measurement by DLR on virgin ZURAM® at 20 K/min in N_2, and the heat capacity of CALCARB® CBCF 18-2000 measured by VKI at 40 K/min in Ar

3.2.11. Heat of pyrolysis U

The heat of pyrolysis is given by the difference between the gas enthalpy and the solid phase enthalpy. VKI will attempt to experimentally set this value through the TGA/DSC measurements on resin, virgin and charred ZURAM® . The value might be updated in the final version of this document.

If the heat of pyrolysis cannot be determined experimentally, a linear evolution of the solid density ρ from the virgin state ρ_v to the charred state ρ_c will be assumed, and the heat of pyrolysis H_p will be numerically computed as defined in the Equation 4:

$$H_p = h^g - \frac{\rho_v \, h_v - \rho_c \, h_c}{\rho_v - \rho_c} \tag{4}$$

where h^g is the gas enthalpy.

3.2.12. Emissivity

The emissivity is 0.8 for virgin ZURAM® , and 0.9 for charred ZURAM® [RD7]. New measurements (in-situ during plasma testing and for virgin using the new emissivity-evaluation setup) will be performed by VKI. The values will be updated in case of inconsistencies.

4. Geometry and boundary conditions

Preliminary remark:
In both 1D and 2D axisymmetric models defined hereafter, all the samples are equally oriented such that the "through-the-thickness" direction lies along z-axis. This orientation is consistent with the orthotropic material properties defined in section 3 (more specifically with the effective thermal conductivities k_{xx}, k_{yy}, k_{zz}).

4.1. One-dimensional planar test cases

4.1.1. Geometry

All the test cases are assumed 1D planar:

- the length of the sample is $L = 50$ mm
- on one side, the sample is heated (at $z = 0$)
- the opposite side is adiabatic and impermeable (as are the lateral sides, since the model is 1D)

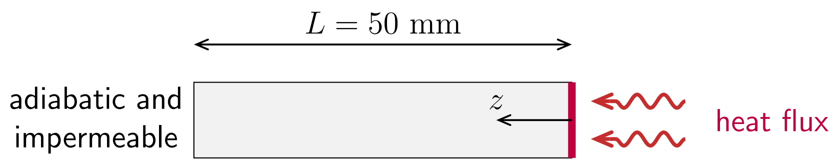

Figure 1: One-dimensional planar numerical test case

4.1.2. Initial conditions

The initial temperature of the sample is uniform and equal to $T_0 = 300$ K

The initial composition of the surrounding gas is Air (mole fractions: O_2=0.21, N_2=0.79) and the initial gas pressure is $P_0 = 50$ hPa

4.1.3. Boundary conditions

Prescribed wall temperature
The first type of heating boundary condition is defined by a prescribed wall temperature T_{w}, with a linear ramp applied during the first 0.1 s from the initial temperature T_0 to

T_w, then constant during the remaining test duration, see Figure 2.

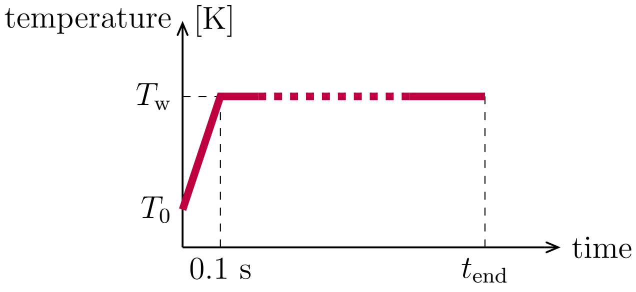

Figure 2: Prescribed wall temperature vs. time

The value of T_{w} could be test-case dependent, but it was chosen equal to 1500 K for all 1D test cases with prescribed wall temperature in this campaign (i.e., Num-1-T-P and Num-1-T-Z).

Convective heat flux and re-radiation

The second type of heating boundary condition is defined by applying a heat flux given by:

$$q_w = \rho_e \, u_e \, C_H \, (H_r - H_w) \tag{5}$$

where $\rho_e u_e C_H$ is the heat transfer coefficient, H_r is the recovery enthalpy and H_w is the gas enthalpy at the wall. Assuming Prandtl number $Pr = 1$, the recovery enthalpy is related to the edge enthalpy H_e as follows:

$$H_r = H_e + \frac{u_e^2}{2} \tag{6}$$

The value of the heat transfer coefficient (the product $\rho_e u_e C_H$), and the recovery enthalpy H_r will be evaluated by the means of aero-thermal calculations, then provided as a boundary condition to the current ablation test cases. The resulting cold-wall heat flux will be approximately:

- low ($\approx$ 0.5 MW/m^2) for the test case Num-2-SEB-Z
- medium ($\approx$ 1.5 MW/m^2) for the test case Num-3-SEB-Z

- high ($\approx$ 5.0 MW/m^2) for the test case Num-4-SEB-Z

The heat transfer coefficient will be kept constant during the heating period (until t = 120 s). After heating, a period of cooling (of the same duration as heating) is modelled by setting the heat transfer coefficient to zero with a linear transition during 0.1 s, see Figure 3.

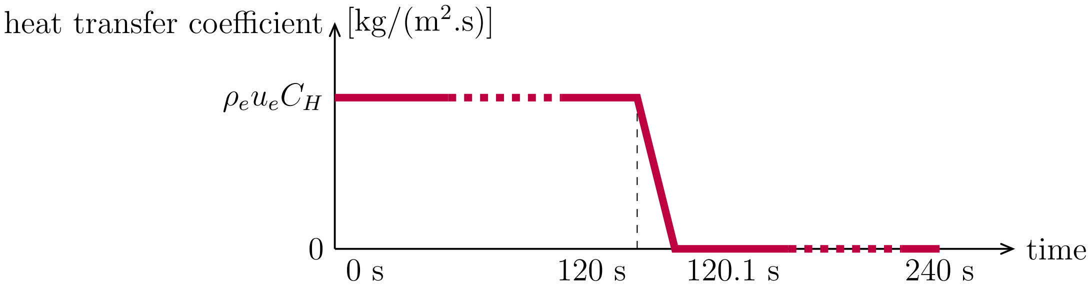

Figure 3: Heat transfer coefficient vs. time

In addition to the applied heat flux, re-radiation is active during the whole test (heating and cooling), considering a view factor equal to 1 and the infinity temperature T_∞ = 300 K. The emissivity of the virgin/charred material is defined in the material properties, cf. section 3.

Additional boundary conditions

The wall pressure P_w is prescribed equal to 50 hPa for all 1D test cases.

When required by the test case definition, the recession speed at wall $\dot{r}_w$ due to ablation must be modelled using the following assumptions:

- The factor for the blowing-correction correlation (CMA-like model) is taken as $\lambda = 0.5$
- Heat and mass transfer coefficients are assumed equal in the boundary layer and $Pr = Le = 1$
- The wall enthalpy h_w and dimensionless ablation speed B'_c are provided as tables in the `Bprime_tables.txt` file as functions of
  - the wall pressure P_w (in a range 0.001–1 bar)
  - the dimensionless out-gassing parameter B'_g (in the range 0–10)
  - the wall temperature T_w (in the range 300–3500 K)

These tables are available for ZURAM® pyrolysis gas in both air and nitrogen atmospheres.

4.1.4. Thermocouples position

For the purpose of code-to-code comparison, a set of specific locations is defined in order to provide time-dependent results (see section 5).

In the case of the 1D tests, these locations will not be confronted to any physical measurement of an experimental campaign. The locations can therefore be defined a priori without taking care of the exact positioning of thermocouples in any real tested sample.

The coordinates of the thermocouples are provided in the Table 7. They apply for all 1D test cases.

z_1	z_2	z_3	z_4	z_5	z_6	z_7	z_8	z_9
0 mm	1 mm	2 mm	4 mm	8 mm	12 mm	16 mm	24 mm	50 mm

Table 7: Coordinates of virtual thermocouples for one-dimensional planar test cases

It must be underlined that z_1 is located on the heated surface ($z_1 = 0$ in time $t = 0$). Later, it is moving with it when recession occurs, i.e. $z_1 = z_w$ (like a pyrometer), while other coordinates are fixed (like thermocouples), z_9 being on the left-end surface.

4.2. Two-dimensional hemispherical test cases

4.2.1. Geometry

Idealized 2D hemisphere

All the 2D test samples (both made of CALCARB® and of ZURAM®) share the same hemispherical-cylindrical axisymmetric geometry. In a first step, an idealized geometry will be considered for all the numerical test cases: the nose radius is $R = 25$ mm, and the sample total length is $L = 40$ mm (cf. Figure 4).

Real geometry

The actual geometry of the 2D samples includes a cylindrical hole in the central part to insert a graphite plug holding the sample in place during the test (see Figure 5).

A more realistic geometry (Figure 6), including the hole and the plug, is intended to be used only in the most advanced modelling, when all the phenomena that can be defined

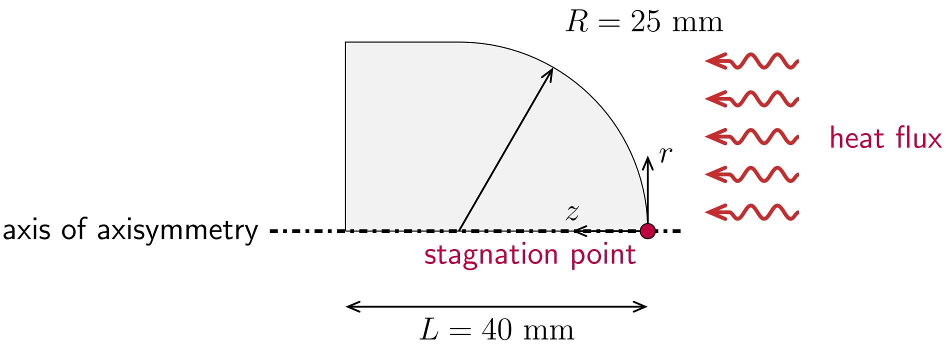

Figure 4: Idealized two-dimensional hemispherical (axisymmetric) test sample

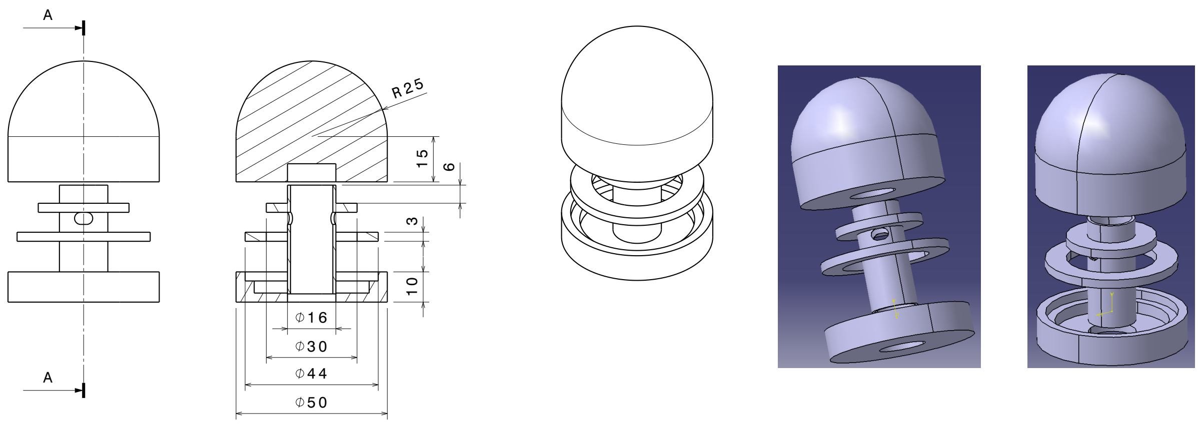

Figure 5: Detailed geometry and CAD rendering of the 2D hemispherical samples and holding plug.

in the thermal response codes are included, i.e. in the re-run of the EXP-3-xxx-P and EXP-5-xxx-Z tests, when the higher fidelity internal radiation is modelled. Before to run these tests with a more advanced model (internal radiation + hole), a first run with simplified geometry (Figure 4) and no internal radiation will be performed, allowing to assess the sensitivity of the response to these parameters. The comparison should be done prior to start the full numerical tests campaign.

To model the realistic geometry, the following (isotropic) material properties of graphite can be used [RD11]:

- density $\rho = 1720$ kg/m^3
- conductivity $k = 92$ W/(m.K)
- heat capacity:

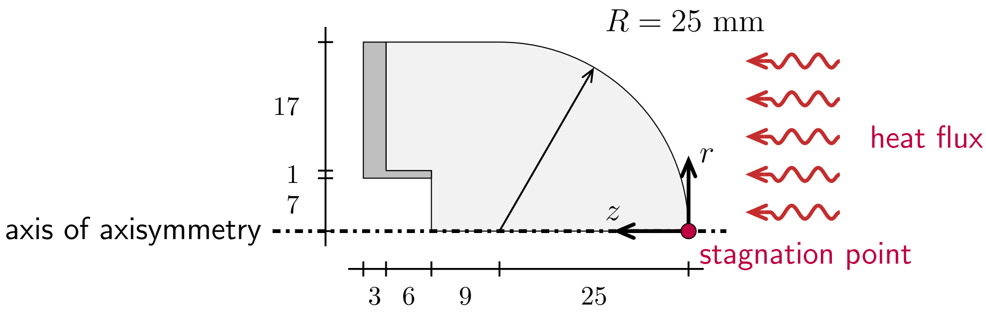

Figure 6: More realistic two-dimensional hemispherical test sample (all dimensions in mm) – Graphite holding plug in dark gray, sample in light gray.

T [K]	500	1000	1500	2000	2500	3000	3500	3700
c_p [J/(kg.K)]	1200	1575	2050	2125	2200	2300	2600	3150

Table 8: Heat capacity of graphite

- emissivity ε =0.94

The boundary conditions around the plug are: perfect contact with the sample and radiative equilibrium inside the plug.

4.2.2. Initial conditions

In a first time, the initial temperature of the sample is uniform and equal to $T_0 = 300$ K. As soon as experimental results will be available, the initial temperature will be updated according to the measurements.

The initial composition of the atmosphere is either air (mol fractions: O_2=0.21, N_2=0.79) or nitrogen (mol fraction: N_2=1).

The initial gas pressure P_0 is set equal to the wall pressure P_w prescribed during the test. This value is case dependent, see section 6.

4.2.3. Boundary conditions

Prescribed wall temperature and recession rate

The first type of boundary condition is prescribing both:

- the wall temperature T_w

- the recession rate $\dot{r}_{\text{w}}$;

The value of T_{w} and $\dot{r}_{\text{w}}$ are test case dependent.

In a first run of numerical test cases, T_{w} is defined as in the detailed description of test cases in section 6 (1500 K, 2500 K, 3000 K). As a first approximation, the wall temperature is applied onto the whole heated surface of the sample. A linear ramping is again assumed during the first 0.1 s, cf. Figure 2.

Later, when the experimental tests results will be available, these temperatures (as well a the recession speed) will be updated. The prescribed wall temperature and surface recession will not be uniform, but it will be consistent with the experimental measurements.

In addition, the cooling phase will also be included in the numerical test cases, as the surface temperature will be available after the experimental measurements.

Convective heat flux and re-radiation

The second type of heating boundary condition is again defined by applying a heat flux given by the Equation 5.

The value of the heat transfer coefficient (the product $\rho_e u_e C_H$), and the recovery enthalpy H_r will also be evaluated by aero-thermal calculations, and provided as boundary conditions. The resulting cold-wall heat flux will be approximately as defined in the section 6: ≈ 0.3 MW/m^2, ≈ 2.5 MW/m^2, or ≈ 4.5 MW/m^2 for supersonic test cases. The evolution in time of the heat transfer coefficient is assumed the same as for the 1D test cases, cf. Figure 3.

Important note: The heat transfer coefficient $\rho_e u_e C_H$ and the recovery enthalpy H_r will be provided at the *stagnation point* (in $r = z = 0$, or in $s = 0$ in curvilinear coordinates along the surface, measured from the pole). These parameters will allow to compute the applied heat flux at stagnation point q_{w0}. In order to extend the boundary condition definition to the full external surface of the samples, a heat flux distribution function $\varphi(s,t)$ must be define to "weight" the applied flux along the sample surface, so that:

$$q_w(s,t) = \varphi(s,t)\, q_{w0(t)} \tag{7}$$

A similar approach was used in the test case series 3 of the 5$^{\text{th}}$ Ablation Workshop [RD3], but for another geometry (iso-q specimens). Moreover, the hemispherical specimens are subjected to an evolution in time of their surface shape, hence an evolution of the distribution function. A linear interpolation in time between the original and the final distributions will be assumed. CFD computations will be performed by VKI once the test conditions are known.

In addition to this applied heat flux, re-radiation is active during the whole test, considering a view factor equal to 1 and the infinity temperature $T_\infty = 300$ K. The emissivity of the virgin/charred material is defined in the material properties, cf. section 3.

Additional boundary conditions

The wall pressure P_w is prescribed during the test. Its value is case dependent, see section 6.

When required by the test case definition, the recession speed at wall $\dot{r}_w$ due to ablation must be modelled using the following assumptions:

- The factor for the blowing-correction correlation (CMA model) is taken as $\lambda = 0.5$
- Heat and mass transfer assumptions in the boundary layer are: $Pr = Le = 1$
- The wall enthalpy h_w and dimensionless ablation speed B'_c are provided as tables in the `Bprime_tables.txt` file as function of
  - the wall pressure P_w (in a range 0.001–1 bar)
  - the dimensionless out-gassing parameter B'_g (in the range 0–10)
  - the wall temperature T_w (in the range 300–3500 K)

  These tables are available for ZURAM® pyrolysis gas in both air and nitrogen atmospheres.

4.2.4. Thermocouples position

For both code-to-code and code-to-experiments comparisons, a set of specific locations are defined in order to provide time-dependent results (see section 5).

Since 2D tests will be performed also experimentally, the exact positioning of the thermocouples will be provided as soon as their actual coordinates will be measured by tomographic analysis (cf. WP 3.1 Plasma Test Plan activity). The coordinates in the numerical tests will be updated then and they will be test-case dependent.

As a first approach, the nominal position of thermocouples can be used for all 2D test cases, see Table 9.

	TC_0	TC_1	TC_2	TC_3	TC_4	TC_5	TC_6	TC_7	TC_8
radial (r)	0 mm	15 mm	10 mm	5 mm	0 mm	5 mm	15 mm	20 mm	15 mm
axial (z)	0 mm	10 mm	7 mm	10 mm	3 mm	15 mm	20 mm	25 mm	40 mm

Table 9: Nominal coordinates of thermocouples for two-dimensional hemispherical test cases

It must be underlined that TC_0 is not a real thermocouple, but located on recession point ($r = z = 0$ in time $t = 0$). Later, it is moving with it when recession occurs, i.e. $r = 0$ and $z = z_w$ (like a pyrometer), while other coordinates are fixed (like thermocouples).

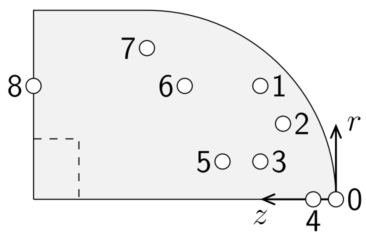

Figure 7: Nominal position of thermocouples in 2D hemispherical samples

5. Output results and file format

5.1. Thermal response

The result files should be named as `CodeName_Energy_TestID.txt` where `TestID` refers to the identification of the test as defined in the section 6, e.g. `Num-3-SEB-Z` or `Exp-5-T-Z`.

The results are the temperature [K] at the specific locations (thermocouples) defined in the Tables 7 and 9, for 1D and 2D test cases, respectively.

The results will be supplied in ASCII files, according to the following format, with an output frequency of 0.1 s:

```
time (s)   Tw (K)   T2 (K)   T3 (K)   T4 (K)   T5 (K)    ...
       0  3.000e2  3.000e2  3.000e2  3.000e2  3.000e2    ...
     0.1  9.651e2  3.225e2  3.000e2  3.000e2  3.000e2    ...
     0.2  1.076e3  3.956e2  3.039e2  3.000e2  3.000e2    ...
    etc.
```

Table 10: Output format for the `CodeName_Energy_TestID.txt` files

5.2. Pyrolysis and ablation response

For each numerical test case involving pyrolysis and/or recession phenomena, three result files should be provided and named:

1. `CodeName_Density_TestID.txt`

The results are the density [kg/m^3] at the specific locations (thermocouples) defined in the Tables 7 and 9, for 1D and 2D test cases, respectively.

The results will be supplied in ASCII files, according to the following format, with an output frequency of 0.1 s:

```
time (s) rhow (kg/m3) rho2 (kg/m3) rho3 (kg/m3) rho4 (kg/m3) rho5 (kg/m3)    ...
       0      4.300e2      4.300e2      4.300e2      4.300e2      4.300e2    ...
     0.1      4.287e2      4.300e2      4.300e2      4.300e2      4.300e2    ...
     0.2      4.255e3      4.300e2      4.300e2      4.300e2      4.300e2    ...
    etc.
```

Table 11: Output format for the `CodeName_Density_TestID.txt` files

2. `CodeName_Mass_TestID.txt`

The results are:

- blowing rates $\dot{m}_g$ [kg/(m^{2}s)] and $\dot{m}_c$ [kg/(m^{2}s)] at the outer surface;
- mass: the total mass [kg] of the specimen;

The results will be supplied in ASCII files, according to the following format, with an output frequency of 0.1 s:

```
time    m_dot_g   m_dot_c       Mass
 (s)  (kg/m2/s)  (kg/m2/s)       (kg)
   0          0          0  2.6736e-2
 0.1   5.063e-3          0  2.6733e-2
 0.2   1.340e-2          0  2.6724e-2
etc.
```

Table 12: Output format for the `CodeName_Mass_TestID.txt` files

3. `CodeName_Recession_TestID.txt`

The results are:

- Pyrolysis zone, i.e. the depth [mm] of the “almost” virgin (98 %) front $z_{\rho_{v^*}}$ and the ”almost” charred (2 %) front $z_{\rho_{c^*}}$, the thresholds being defined as:

$$\rho_{v^*} = \rho_c + 0.98(\rho_v - \rho_c) \tag{8}$$

$$\rho_{c^*} = \rho_c + 0.02(\rho_v - \rho_c) \tag{9}$$

  where the densities ρ_i are the ones of the composite material (not the intrinsic densities of the virgin/charred resin).
  For the sake of simplicity, the depth of these two fronts is measured from the initial outer surface.
  In 2D test cases, these two fronts are measured along the axis of symmetry (depth from the recession point).

- Surface recession, i.e. the coordinate(s) [mm] of of some reference points on the receding surface:
  - In 1D test cases, the reference point is simply on the external heated surface, and the required output is the z-coordinate of the recession surface.
  - In 2D test cases, the reference points are defined as the intersection P_j between the recession surface and straight lines from the center O of the hemisphere circular base pointing in the direction α_j (see Figure 8), where

$\alpha_j \in \{0°, 15°, 30°, 45°, 60°, 75°, 90°\}$. Two additional points P_A and P_B are defined to track the surface geometry evolution in the cylindrical part at mid-height of the cylinder ($z_A = 0.0325$ m) and at the "bottom" surface ($z_B = 0.04$ m), respectively (see Figure 8).

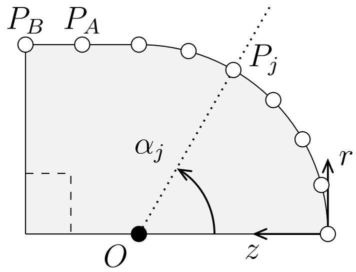

Figure 8: Position of the recession measurement points (for the 2D hemisphere test cases)

The results will be supplied in ASCII files, according to the following format, with an output frequency of 0.1 s.

For the 1D test cases:

time	z_virg98	z_char2	z_0
(s)	(m)	(m)	(m)
0	0	0	0
0.1	0	0	0
0.2	1.781e-4	2.130e-5	0
etc.			

Table 13: Output format for the `CodeName_Recession_TestID.txt` files (1D test cases).

For the 2D test cases, only the z-coordinate of $P_{0°}$ and the r-coordinate of $P_{90°}$, P_A and P_B make sense:

time	z_virg98	z_char2	z_0	r_15	z_15	...	r_90	r_A	r_B
(s)	(m)	(m)	(m)	(m)	(m)	...	(m)	(m)	(m)
0	0	0	0	6.470e-1	8.852e-2	...	2.5e-3	2.5e-3	2.5e-3
0.1	0	0	0	6.470e-1	8.852e-2	...	2.5e-3	2.5e-3	2.5e-3
0.2	1.781e-4	2.130e-5	0	6.470e-1	8.852e-2	...	2.5e-3	2.5e-3	2.5e-3
etc.									

Table 14: Output format for the `CodeName_Recession_TestID.txt` files (2D test cases).

6. Detailed description of the numerical test cases

6.1. 1D planar test cases

Num-1-T-P

This test is a simple 1D thermal analysis test with imposed boundary conditions. Because CALCARB® will be used, the pyrolysis effect and gas mass flow will not be present, and it is the simplest test one can perform with a thermal response code. The goal of this test is to complete the **Num-i-j-k** series, and prepare a CALCARB® thermal model, which will be used also in the test campaign.

Included physical phenomena:

✓ λ_c

Numerical test conditions:

Test ID	Num-1-T-P
Plasm. exp.	–
Geometry	1D planar
Material	CALCARB®
Cold-wall heat flux	–
Gas	–
BC	T_{w}
Duration	120 s
Max T_w	1500 K
P_w	50 hPa

Requested output results:

✓ thermal response

Num-1-T-Z

This numerical example comes from the 4^{th} Ablation Work Shop [RD1] for code comparison. The goal of this 1D example is to test the basic functionalities of a charring-ablator code, while at the same time avoiding the interaction between the balance equations on the one side and boundary conditions and mesh deformation (due to ablation) on the other. The example tests heat transfer, pyrolysis decomposition and unidirectional gas transfer.

Included physical phenomena:

- ✓ λ_c
- ✓ λ_v
- ✓ pyrolysis
- ✓ convective heat transfer

Numerical test conditions:

Test ID	Num-1-T-Z
Plasm. exp.	–
Geometry	1D planar
Material	ZURAM®
Cold-wall heat flux	–
Gas	–
BC	T_{w}
Duration	120 s
Max T_w	1500 K
P_w	50 hPa

Requested output results:

- ✓ thermal response
- ✓ density (TC)
- ✓ blowing rate
- ✓ pyrolysis zone
- ✓ mass

Num-2-SEB-Z

During the 5^{th} Ablation Workshop [RD2], the simple numerical test **Num-1-T-Z** was extended, in order to include all relevant phenomena for charring ablators, defining tests of increasing complexity **Num-i-SEB-Z**. This test uses the SEB, but not yet surface ablation, thus modelling only the interaction between the balance equations and the boundary conditions.

Included physical phenomena:

- ✓ λ_c
- ✓ λ_v
- ✓ pyrolysis
- ✓ convective heat transfer
- ✓ oxidation

Numerical test conditions:

Test ID	Num-2-SEB-Z
Plasm. exp.	–
Geometry	1D planar
Material	ZURAM®
Cold-wall heat flux	0.5 MW/m^2
Gas	Air
BC	SEB
Duration	120 s
Est. Max T_w	1500 K
P_w	50 hPa

Requested output results:

- ✓ thermal response
- ✓ density (TC)
- ✓ blowing rate
- ✓ pyrolysis zone
- ✓ mass

Num-3-SEB-Z

In the second numerical test of the 5^{th} Ablation Workshop the surface recession was added, and all the phenomena were therefore activated. The recession rate was still moderate, in order for the code developers to find problems with the interaction between mesh deformation (due to recession) and the solution of the balance equations.

Included physical phenomena:

- ✓ λ_c
- ✓ λ_v
- ✓ pyrolysis
- ✓ convective heat transfer
- ✓ oxidation
- ✓ recession

Numerical test conditions:

Test ID	Num-3-SEB-Z
Plasm. exp.	–
Geometry	1D planar
Material	ZURAM®
Cold-wall heat flux	1.5 MW/m^2
Gas	Air
BC	SEB
Duration	120 s
Est. Max T_w	1500 K
P_w	50 hPa

Requested output results:

- ✓ thermal response
- ✓ density (TC)
- ✓ blowing rate
- ✓ pyrolysis zone
- ✓ surface recession
- ✓ mass

Num-4-SEB-Z

In the final numerical test of the 5^{th} Ablation Workshop, all phenomena were activated and the heat flux was chosen such to be representative of a high heat flux condition with high ablation (sublimation regime). This example tests the interaction between all phenomena of a thermal response code for charring ablators.

Included physical phenomena:

- ✓ λ_c
- ✓ λ_v
- ✓ pyrolysis
- ✓ convective heat transfer
- ✓ oxidation
- ✓ sublimation
- ✓ recession

Numerical test conditions:

Test ID	Num-4-SEB-Z
Plasm. exp.	–
Geometry	1D planar
Material	ZURAM®
Cold-wall heat flux	5.0 MW/m^2
Gas	Air
BC	SEB
Duration	120 s
Est. Max T_w	3000 K
P_w	50 hPa

Requested output results:

- ✓ thermal response
- ✓ density (TC)
- ✓ blowing rate
- ✓ pyrolysis zone
- ✓ surface recession
- ✓ mass

6.2. 2D axisymmetric test cases – Low heat flux

Exp-1-T-P/Exp-1-SEB-P

The objective is to test the CALCARB® for low heat flux conditions in an N_2 environment. No recession will take place and the only variables will be the thermal properties of CALCARB® . Because the properties given by the supplier have a high variability these tests are used to perform a sensitivity study on the conductivity, and obtain the correct properties by performing a regression analysis. Two types of boundary conditions are tested, allowing the separation of boundary conditions from the volume balance equations.

Included physical phenomena:

- ✓ 2D effects
- ✓ λ_v

Numerical tests conditions:

Test ID	Exp-1-T-P
Plasm. exp.	P-N-50-q300
Geometry	2D hemisphere
Material	CALCARB®
Cold-wall heat flux	0.3 MW/m^2
Gas	N_2
BC	T_w, $\dot{r}$
Duration	120 s
Max T_w	1500 K
P_w	50 hPa

Test ID	Exp-1-SEB-P
Plasm. exp.	P-N-50-q300
Geometry	2D hemisphere
Material	CALCARB®
Cold-wall heat flux	0.3 MW/m^2
Gas	N_2
BC	SEB
Duration	120 s
Est. Max T_w	1500 K
P_w	50 hPa

Requested output results:

- ✓ thermal response

Exp-2-T-Z/Exp-2-SEB-Z

A fully instrumented set of tests with ZURAM® in an Air environment and low heat flux levels is performed. This will add the effect of pyrolysis and oxidation at the surface, w.r.t. to the previous tests. Two types of boundary conditions are tested, allowing the separation of boundary conditions from the volume balance equations.

Included physical phenomena:

- ✓ 2D effects
- ✓ λ_c
- ✓ λ_v
- ✓ pyrolysis
- ✓ convective heat transfer
- ✓ oxidation

Numerical tests conditions:

Test ID	Exp-2-T-Z
Plasm. exp.	Z-A-50-q300
Geometry	2D hemisphere
Material	ZURAM®
Cold-wall heat flux	0.3 MW/m^2
Gas	Air
BC	T_w, $\dot{r}$
Duration	120 s
Max T_w	1500 K
P_w	50 hPa

Test ID	Exp-2-SEB-Z
Plasm. exp.	Z-A-50-q300
Geometry	2D hemisphere
Material	ZURAM®
Cold-wall heat flux	0.3 MW/m^2
Gas	Air
BC	SEB
Duration	120 s
Est. Max T_w	1500 K
P_w	50 hPa

Requested output results:

- ✓ thermal response
- ✓ density (TC)
- ✓ blowing rate
- ✓ pyrolysis zone
- ✓ surface recession
- ✓ mass

6.3. 2D hemispherical test cases – High heat flux

Exp-3-T-P/Exp-3-SEB-P

The conductivity properties found during the test case **Exp-1-T-P/Exp-1-SEB-P**, are used here in order to validate these properties for the high heat flux case. Because of the porous nature of CALCARB®, these two tests could potentially show the effect of non-Rosseland type of radiation behaviour, i.e. faster heating up of the deeper lying thermocouples.

Included physical phenomena:

- ✓ 2D effects
- ✓ λ_c
- ✓ recession
- ✓ non-equilibrium radiation (re-run with higher fidelity internal radiation model)

Numerical tests conditions:

Test ID	Exp-3-T-P
Plasm. exp.	P-N-100-q2500
Geometry	2D hemisphere
Material	CALCARB®
Cold-wall heat flux	2.5 MW/m^2
Gas	N_2
BC	T_w, $\dot{r}$
Duration	34 s
Max T_w	2500 K
P_w	100 hPa

Test ID	Exp-3-SEB-P
Plasm. exp.	P-N-100-q2500
Geometry	2D hemisphere
Material	CALCARB®
Cold-wall heat flux	2.5 MW/m^2
Gas	N_2
BC	SEB
Duration	34 s
Est. Max T_w	2500 K
P_w	100 hPa

Requested output results:

- ✓ thermal response
- ✓ density (TC)
- ✓ blowing rate
- ✓ pyrolysis zone
- ✓ surface recession
- ✓ mass

Exp-3-T-Z/Exp-3-SEB-Z

A fully instrumented set of tests with ZURAM® in an N_2 environment and high heat flux levels is performed. This will add the pyrolysis effect, w.r.t. to the previous tests. Two types of boundary conditions are tested, allowing the separation of boundary conditions from the volume balance equations.

Included physical phenomena:

- ✓ 2D effects
- ✓ λ_c
- ✓ λ_v
- ✓ pyrolysis
- ✓ convective heat transfer
- ✓ recession

Numerical tests conditions:

Test ID	Exp-3-T-Z
Plasm. exp.	Z-N-100-q2500
Geometry	2D hemisphere
Material	ZURAM®
Cold-wall heat flux	2.5 MW/m^2
Gas	N_2
BC	T_w, $\dot{r}$
Duration	30 s
Max T_w	2500 K
P_w	100 hPa

Test ID	Exp-3-SEB-Z
Plasm. exp.	Z-N-100-q2500
Geometry	2D hemisphere
Material	ZURAM®
Cold-wall heat flux	2.5 MW/m^2
Gas	N_2
BC	SEB
Duration	30 s
Est. Max T_w	2500 K
P_w	100 hPa

Requested output results:

- ✓ thermal response
- ✓ density (TC)
- ✓ blowing rate
- ✓ pyrolysis zone
- ✓ surface recession
- ✓ mass

Exp-4-T-Z/Exp-4-SEB-Z

This set of tests (high heat flux level), extends the **Exp-3-T-Z/Exp-3-SEB-Z** tests to include oxidation due to the Air environment. Two types of boundary conditions are tested, allowing the separation of boundary conditions from the volume balance equations.

Included physical phenomena:

- ✓ 2D effects
- ✓ λ_c
- ✓ λ_v
- ✓ pyrolysis
- ✓ convective heat transfer
- ✓ oxidation
- ✓ recession

Numerical tests conditions:

Test ID	Exp-4-T-Z
Plasm. exp.	Z-A-100-q2500
Geometry	2D hemisphere
Material	ZURAM®
Cold-wall heat flux	2.5 MW/m^2
Gas	Air
BC	T_w, $\dot{r}$
Duration	30 s
Max T_w	2500 K
P_w	100 hPa

Test ID	Exp-4-SEB-Z
Plasm. exp.	Z-A-100-q2500
Geometry	2D hemisphere
Material	ZURAM®
Cold-wall heat flux	2.5 MW/m^2
Gas	Air
BC	SEB
Duration	30 s
Est. Max T_w	2500 K
P_w	100 hPa

Requested output results:

- ✓ thermal response
- ✓ density (TC)
- ✓ blowing rate
- ✓ pyrolysis zone
- ✓ surface recession
- ✓ mass

6.4. 2D hemispherical test cases – Supersonic conditions

Exp-5-T-Z/Exp-5-SEB-Z

These tests extend the range of the flow to supersonic conditions. This will result in higher heat flux levels and higher recession rates leading to shape change of the sample surface. These tests will include all the phenomena that can be modelled in the thermal response codes.

Included physical phenomena:

- ✓ 2D effects
- ✓ λ_c
- ✓ λ_v
- ✓ pyrolysis
- ✓ convective heat transfer
- ✓ oxidation
- ✓ sublimation
- ✓ recession
- ✓ shape change
- ✓ non-equilibrium radiation (re-run with higher fidelity internal radiation model)

Numerical tests conditions:

Test ID	Exp-5-T-Z
Plasm. exp.	SS-Z-A
Geometry	2D hemisphere
Material	ZURAM®
Cold-wall heat flux	4.5 MW/m^2
Gas	Air
BC	T_w, $\dot{r}$
Duration	TBD
Max T_w	3000 K
P_w	TBD

Test ID	Exp-5-SEB-Z
Plasm. exp.	SS-Z-A
Geometry	2D hemisphere
Material	ZURAM®
Cold-wall heat flux	4.5 MW/m^2
Gas	Air
BC	SEB
Duration	TBD
Est. Max T_w	3000 K
P_w	TBD

Requested output results:

- ✓ thermal response
- ✓ density (TC)

- ✓ blowing rate
- ✓ pyrolysis zone
- ✓ surface recession
- ✓ mass

A. Tacot_Zuram_Calcarb_database.ods: TACOT 3.0

Material: TACOT 3.0 [2]

Description

Theoretical material from Ablation Workshop test case. Created to mimic Pica.

Material characteristics

Charring:	YES
Isotropy	Isotropic

Volume fraction [-]

	Gas	Fibers	Resin
Virgin	8.00E-001	1.00E-001	1.00E-001
Char	8.50E-001	1.00E-001	5.00E-002

Average density [kg/m³]

Virgin	Charred
2.80E+002	2.20E+002

Intrinsic density [kg/m³]

Fibers	Resin matrix
1.60E+003	1.20E+003

Permeability [m²]

Virgin	Charred
1.60E-11	2.00E-11

Tortuosity [-]

Virgin	Charred
1.20E+00	1.10E+00

Solid phase heat capacity [5]

Solid phases heat capacity [J/kg/K]

Temperature [K]	Virgin	Charred
2.56E+002	8.79E+002	7.33E+002
2.98E+002	9.84E+002	7.83E+002
4.44E+002	1.30E+003	1.09E+003
5.56E+002	1.47E+003	1.32E+003
6.44E+002	1.57E+003	1.43E+003
8.33E+002	1.72E+003	1.67E+003
1.11E+003	1.86E+003	1.84E+003
1.39E+003	1.93E+003	1.97E+003
1.67E+003	1.98E+003	2.05E+003
1.94E+003	1.99E+003	2.09E+003
2.22E+003	2.00E+003	2.11E+003
2.78E+003	2.01E+003	2.14E+003
3.33E+003	2.01E+003	2.15E+003

Effective conductivity [5]

Through-the-thickness [W/m/K]

Temperature [K]	Virgin	Charred
2.56E+002	3.98E-001	3.98E-001
2.98E+002	4.02E-001	4.02E-001
4.44E+002	4.16E-001	4.16E-001
5.56E+002	4.53E-001	4.53E-001
6.44E+002	4.70E-001	4.70E-001
8.33E+002	4.86E-001	4.86E-001
1.11E+003	5.23E-001	5.23E-001
1.39E+003	5.60E-001	5.60E-001
1.67E+003	6.98E-001	6.05E-001
1.94E+003	8.72E-001	7.29E-001
2.22E+003	1.11E+000	9.22E-001
2.78E+003	1.75E+000	1.46E+000
3.33E+003	2.78E+000	2.32E+000

In-plane [W/m/K]

Temperature [K]	Virgin	Charred

2.56E+002	3.98E-001	3.98E-001
2.98E+002	4.02E-001	4.02E-001
4.44E+002	4.16E-001	4.16E-001
5.56E+002	4.53E-001	4.53E-001
6.44E+002	4.70E-001	4.70E-001
8.33E+002	4.86E-001	4.86E-001
1.11E+003	5.23E-001	5.23E-001
1.39E+003	5.60E-001	5.60E-001
1.67E+003	6.98E-001	6.05E-001
1.94E+003	8.72E-001	7.29E-001
2.22E+003	1.11E+000	9.22E-001
2.78E+003	1.75E+000	1.46E+000
3.33E+003	2.78E+000	2.32E+000

	In-plane [W/m/K]	
Temperature [K]	**Virgin**	**Charred**
2.56E+002	3.98E-001	3.98E-001
2.98E+002	4.02E-001	4.02E-001
4.44E+002	4.16E-001	4.16E-001
5.56E+002	4.53E-001	4.53E-001
6.44E+002	4.70E-001	4.70E-001
8.33E+002	4.86E-001	4.86E-001
1.11E+003	5.23E-001	5.23E-001
1.39E+003	5.60E-001	5.60E-001
1.67E+003	6.98E-001	6.05E-001
1.94E+003	8.72E-001	7.29E-001
2.22E+003	1.11E+000	9.22E-001
2.78E+003	1.75E+000	1.46E+000
3.33E+003	2.78E+000	2.32E+000

Thermochemistry [5]

Enthalpy of formation at 298K [J/kg]	
Char	0
Phenolic resin	-2.000E+06
Virgin	-8.571E+05

Pyrolysis kinetics [1]

$f_j(\xi_j, T) = (1-\xi_j)^{m_j} T^{n_j} \mathcal{A}_j \exp\left(-\frac{\mathcal{E}_j}{\mathcal{R}T}\right.$

Number of pseudo-phases	2
Number of reactions	2

SI units	**Density loss fraction**		**Arrhenius parameters**			**Threshold temp.**	**Enthalpy**
Reaction	**f [-]**	**A [SI]**	**E/R [K]**	**m [-]**	**n [-]**	**T0 [K]**	**h [J/kg]**
1	2.500E-01	1.200E+04	8.56E+003	3	0	3.33E+002	-4.00E+006
2	2.500E-01	4.480E+09	2.04E+004	3	0	5.56E+002	-4.00E+006

Average elemental composition of the pyrolysis gases [3]

Element	**Mole fraction**
C	0.206
H	0.679
O	0.115
N	0
Total	1

Initial average molar composition of the pyrolysis gases

Species	CO2	CO	C6H6	C6H5OH	CH4	H2O	H2
Molar fraction	1.57E-002	5.76E-002	4.79E-003	8.91E-002	1.00E-001	2.34E-001	4.99E-001
Mass fraction	3.77E-002	8.82E-002	4.40E-002	4.58E-001	8.75E-002	2.30E-001	5.46E-002

Pyrolysis gas chemical mechanism [4]

File	./Additional_data/TACOT/April1971.
Format	CHEMKIN

Surface radiative properties

	Emissivity
Virgin	0.8
Char	0.9

TACOT datasheet related references:

[1] H.W. Goldstein (1969). Pyrolysis kinetics of nylon 66, phenolic resin, and their composites, J. Macromole. Sci. Part A 3 (4) (1969) 649673
[2] ./Additional_data/TACOT/TACOT_3.0.xls
[3] Sykes, G. F. (1967). Decomposition characteristics of a char-forming phenolic polymer used for ablative composites (No. TN D-3810)
[4] April, G. (1969). Energy Transfer in the char Zone of a Charring Ablator. PhD Thesis, Department of Chemical Engineering, Louisiana State University
[5] Covington, M. A., Heinemann, J. M., Goldstein, H. E., Chen, Y. K., Terrazas-Salinas, I., Balboni, J. A., ... Martinez, E. R. (2008). Performance of a Low Density Ablative Heat Shield Material. Journal of Spacecraft and Rockets, 45(2), 237-247

B. Tacot_Zuram_Calcarb_database.ods: CALCARB®

Material: Calcarb® CBCF 18/2000

Description

Mersen Calcarb Preform (CBCF 18/2000)

Material characteristics

Charring: NO

Isotropy Orthotropic

Volume fraction [-]

Gas	Fibers
8.90E-001	1.10E-001

Average density [kg/m³]

1.80E+002

Intrinsic density [kg/m³]

Fibers
1.64E+003

Permeability [m²]

5.95E-013

Tortuosity [-]

1.10E+00

Solid phase heat capacity [1]

Solid phases heat capacity [J/kg/K]

Temperature [K]	
2.56E+002	4.23E+002
2.98E+002	6.49E+002
4.44E+002	1.10E+003
5.56E+002	1.30E+003
6.44E+002	1.41E+003
8.33E+002	1.57E+003
1.11E+003	1.72E+003
1.17E+003	1.75E+003
1.39E+003	1.83E+003
1.67E+003	1.91E+003
1.94E+003	1.98E+003
2.22E+003	2.05E+003
2.78E+003	2.15E+003
3.33E+003	2.25E+003

Effective conductivity [2]

Through-the-thickness [W/m/K]

Temperature [K]	
2.56E+002	3.98E-001
2.98E+002	4.12E-001
4.44E+002	4.65E-001
5.56E+002	5.09E-001
6.44E+002	5.48E-001

8.33E+002	6.40E-001
1.11E+003	7.96E-001
1.17E+003	8.35E-001
1.39E+003	9.79E-001
1.67E+003	1.19E+000
1.94E+003	1.42E+000
2.22E+003	1.69E+000
2.78E+003	2.29E+000
3.33E+003	3.00E+000

Temperature [K]	**In-plane [W/m/K]**
2.56E+002	1.38E+000
2.98E+002	1.42E+000
4.44E+002	1.53E+000
5.56E+002	1.59E+000
6.44E+002	1.62E+000
8.33E+002	1.62E+000
1.11E+003	2.00E+000
1.17E+003	1.99E+000
1.39E+003	1.91E+000
1.67E+003	1.87E+000
1.94E+003	1.93E+000
2.22E+003	2.08E+000
2.78E+003	2.58E+000
3.33E+003	3.29E+000

Temperature [K]	**In-plane [W/m/K]**
2.56E+002	1.38E+000
2.98E+002	1.42E+000
4.44E+002	1.53E+000
5.56E+002	1.59E+000
6.44E+002	1.62E+000
8.33E+002	1.62E+000
1.11E+003	2.00E+000
1.17E+003	1.99E+000
1.39E+003	1.91E+000
1.67E+003	1.87E+000
1.94E+003	1.93E+000
2.22E+003	2.08E+000
2.78E+003	2.58E+000
3.33E+003	3.29E+000

Surface radiative properties [5]
Emissivity
0.85-0.9

[1] Thermal characterization of ablative materials, Short Training Program Report, F. Torres, VKI, Carbon preform (CBCF 18-2000) heat capacity data from DSC analysis

[2] Calcarb: rigid carbon thermal insulation, Technical guide, , Mersen Scotland Holytown Ltd., Thermal conductivity data on CBCF 18-2000

[3] ZURAM material_data_update.xlsx, Excel file, DLR, Collection of several data for ZURAM (e.g., volume fractions, densities)

[4] TACOT_3.0.xls, Excel file, J. Lachaud, T. van Eekelen, D. Bianchi, A. Martin, , Fictitious material properties from US Ablation Workshop (2014)

[5] Measurement techniques data processing: Relating and contributing to WP2, Ablacat Project, TN-2.4 of ESA AO/1-7664/13/NL/RA, A.Turchi, A. Viladegut, D. Le Quang, B. Helber, O. Chazot, VKI, Emissivity measurements based on pyrometer and radiometer measurements. Range of values from single-color temperature measurements of pyrometer are used.

Remark

There are three principal directions for thermal conductivity (orthotropic material), but two of them (in-plane) are equal (transverse isotropy).

C. Tacot_Zuram_Calcarb_database.ods: ZURAM®

Material: ZURAM® 18/50

Description

Carbon-phenolic ablator produced by DLR. Composed by Mersen Calcarb Preform (CBCF 18/2000) impregnated with phenolic resin.

Material characteristics

Charring:	YES
Isotropy	Orthotropic

Volume fraction [-]

	Gas	Fibers	Resin
Virgin	5.56E-001	1.10E-001	3.34E-001
Char	7.08E-001	1.10E-001	1.82E-001

Average density [kg/m³]

Virgin	Charred
4.30E+002	3.44E+002

Intrinsic density [kg/m³]

Fibers	Virgin Resin matrix	Charred resin matrix
1.64E+003	7.48E+002	8.99E+002

Permeability [m²]

Virgin	Charred
2.31E-013	5.95E-013

Tortuosity [-]

Virgin	Charred
1.20E+00	1.10E+00

Solid phase heat capacity [2] & [4]

Solid phases heat capacity [J/kg/K]

Temperature [K]	Decomposing	Charred [1]
2.56E+002	6.72E+001	4.23E+002
2.98E+002	7.86E+002	6.49E+002
4.44E+002	2.42E+003	1.10E+003
5.56E+002	2.90E+003	1.30E+003
6.44E+002	2.93E+003	1.41E+003
8.33E+002	2.34E+003	1.57E+003
1.11E+003	1.59E+003	1.72E+003
1.17E+003	1.75E+003	1.75E+003
1.39E+003	1.83E+003	1.83E+003
1.67E+003	1.91E+003	1.91E+003
1.94E+003	1.98E+003	1.98E+003
2.22E+003	2.05E+003	2.05E+003
2.78E+003	2.15E+003	2.15E+003
3.33E+003	2.25E+003	2.25E+003

Effective conductivity [2] & [4]

Through-the-thickness [W/m/K]

Temperature [K]	Decomposing	Charred
2.56E+002	1.22E-001	1.09E-001
2.98E+002	2.02E-001	1.63E-001
4.44E+002	4.12E-001	2.65E-001
5.56E+002	5.05E-001	3.10E-001
6.44E+002	5.37E-001	3.43E-001
8.33E+002	4.82E-001	4.21E-001

1.11E+003	4.69E-001	4.69E-001
1.17E+003	4.95E-001	4.95E-001
1.39E+003	6.27E-001	6.27E-001
1.67E+003	8.87E-001	8.87E-001
1.94E+003	1.25E+000	1.25E+000
2.22E+003	1.71E+000	1.71E+000
2.78E+003	2.94E+000	2.94E+000
3.33E+003	4.58E+000	4.58E+000

	In-plane [W/m/K]	
Temperature [K]	Decomposing	Charred
2.56E+002	5.87E-001	3.77E-001
2.98E+002	8.27E-001	5.62E-001
4.44E+002	1.46E+000	8.74E-001
5.56E+002	1.75E+000	9.68E-001
6.44E+002	1.87E+000	1.01E+000
8.33E+002	1.75E+000	1.06E+000
1.11E+003	1.18E+000	1.18E+000
1.17E+003	1.18E+000	1.18E+000
1.39E+003	1.23E+000	1.23E+000
1.67E+003	1.40E+000	1.40E+000
1.94E+003	1.69E+000	1.69E+000
2.22E+003	2.11E+000	2.11E+000
2.78E+003	3.32E+000	3.32E+000
3.33E+003	5.02E+000	5.02E+000

	In-plane [W/m/K]	
Temperature [K]	Decomposing	Charred
2.56E+002	5.87E-001	3.77E-001
2.98E+002	8.27E-001	5.62E-001
4.44E+002	1.46E+000	8.74E-001
5.56E+002	1.75E+000	9.68E-001
6.44E+002	1.87E+000	1.01E+000
8.33E+002	1.75E+000	1.06E+000
1.11E+003	1.18E+000	1.18E+000
1.17E+003	1.18E+000	1.18E+000
1.39E+003	1.23E+000	1.23E+000
1.67E+003	1.40E+000	1.40E+000
1.94E+003	1.69E+000	1.69E+000
2.22E+003	2.11E+000	2.11E+000
2.78E+003	3.32E+000	3.32E+000
3.33E+003	5.02E+000	5.02E+000

$$\prod = -\frac{\partial(\epsilon_m \rho_m)}{\partial t} = \epsilon_{m,0}\rho_{m,0} \sum_{i=1}^{N} F_i$$

$$\frac{\partial \xi_i}{\partial t} = (1-\xi_i)^{n_i} A_i \left(\exp\frac{-E_i}{RT}\right)$$

Thermochemistry [8]

	Enthalpy of formation at 298 K [J/kg]
Char	0
Phenolic resin	-2.000E+06
Virgin	-1.163E+06

Pyrolysis kinetics [3]

Number of pseudo-phases 2 : resin (decomposing to char); fibers (not decomposing)
Number of reactions 3

SI units	**Density loss fraction**	**Arrhenius parameters**		
Reaction	**F [-]**	**A [SI]**	**E/R [K]**	**n [-]**
1	3.500E-02	6.667E+04	8.58E+003	5
2	2.900E-02	8.256E+05	1.33E+004	2.9
3	1.470E-01	9.499E+03	1.20E+004	2.2

Average elemental composition of the pyrolysis gases, from [12] (“Char yield” sheet) using data from [3]

Element	**Mole fraction**	**Mass fraction**	**Molar mass**
C	0.124562099	0.352	12.0107
H	0.750579839	0.178	1.00794
O	0.124858063	0.47	15.999
Total	1		

Surface radiative properties [7]

	Emissivity
Virgin	0.8
Char	0.9

ZURAM® datasheet related references:

[1] Zuram_aged_data_en.xlsx., Excel file, DLR, Thermal diffusivity measurements for ZURAM precharred at different temperatures

[2] Zuram_thermal_conductivity_v2.1, Excel/Openoffice file, VKI, Educated guess of thermal conductivity (and heat capacity) for decomposing ZURAM based on a VKI procedure that accounts for data available from different sources.

[3] Experimental characterization of pyrolysis phenomenon: from carbon composite ablators to Pacific Islands plant biomass, Research Master Report, F. Torres, VKI, TGA measurement of ZURAM

[4] Thermal characterization of ablative materials, Short Training Program Report, F. Torres, VKI, Carbon preform (CBCF 18-2000) heat capacity data from DSC analysis

[5] Calcarb: rigid carbon thermal insulation, Technical guide, Mersen Scotland Holytown Ltd., Thermal conductivity data on CBCF 18-2000

[6] ZURAM material_data_update.xlsx, Excel file, DLR, Collection of several data for ZURAM (e.g., volume fractions, densities)

[7] TACOT_3.0.xls, Excel file, J. Lachaud, T. van Eekelen, D. Bianchi, A. Martin, Fictitious material properties from US Ablation Workshop (2014)

[8] Performance of a Low Density Ablative Heat Shield Material, Journal of Spacecraft and Rockets, 45(2), M. A. Covington et al.

[9] ZURAM material_data_update_VKI.xlsx, Excel file, DLR / modified by VKI, Same as ZURAM material_data_update.xlsx but with modified computation of resin volume fraction and density of char measured by VKI

Remarks

- There are three principal directions for thermal conductivity (orthotropic material), but two of them (in-plane) are equal (transverse isotropy).
- For the thermal diffusivity of partially charred ZURAM® , 30 K steps were used for ZURAM® pre-charred at 300 K & 530 K, and 50 K steps for ZURAM® pre-charred at 600 K & 900 K.

D. Mutation++ input files for B' tables

Mutation++ input file for the generation of the following B' tables in **air atmosphere**.

```
<mixture thermo_db="NASA-9" state_model="EquilTP" mechanism="none">

<species>
C(gr) C H O N CH CH4 CO CO2 CN C2H C2H2,vinylidene C3 C3H C4 C4H
C4H2,butadiyne C5 HCN H2 H2O N2 </species>

<element_compositions>
<composition name="VKIZuramPyroGas">    C:0.125, H:0.750, O:0.125, N:0.
    </composition>
<composition name="BLedge"> C:0., H:0., O:0.21, N:0.79  </composition>
<composition name="Char">   C:1., H:0., O:0., N:0.  </composition>
</element_compositions>
</mixture>
```

Mutation++ input file for the generation of the following B' tables in **nitrogen atmosphere**.

```
<mixture thermo_db="NASA-9" state_model="EquilTP" mechanism="none">

<species>
C(gr) C H O N CH CH4 CO CO2 CN C2H C2H2,vinylidene C3 C3H C4 C4H
C4H2,butadiyne C5 HCN H2 H2O N2 </species>

<element_compositions>
<composition name="VKIZuramPyroGas">    C:0.125, H:0.750, O:0.125, N:0.
    </composition>
<composition name="BLedge"> C:0., H:0., O:0.0 N:1.0  </composition>
<composition name="Char">   C:1., H:0., O:0., N:0.  </composition>
</element_compositions>
</mixture>
```

An example script that uses one of the above mixture files to generate B' tables through the `bprime` command of Mutation++ is the following.

```
#!/bin/bash

# Example of bash script to call recursively the "brime" function of
    Mutation++ and generate B' tables.
# After proper installation of M++ and creation of a mixture file with
    the name of the below "mixture" variable (check mixture using
```

```bash
# the "checkmix" option of Mutation++; this script can be called passing as single parameter the name of the global output file (ex. "./brime_VKI_bash.sh output_file.dat")

# Output of the script
# 1) Global output file (see below) including tables for all the selected pressures and B'g
# 2) Separate files, one for each pressure and B'g, named "p_${pressure}_Bpg_${bp_g}.dat" (where ${pressure} and ${bp_g} are the current pressure and B'g, respectively).

# Global output file name passed as a parameter from command line
out=$1

# Mixture name
mixture=carbonPhenolInAir

# Pyrolysis gas elemental composition name
pyro=VKIZuramPyroGas # As evaluated in Ablantis TN-1 based on Torres (TGA) char density

# Pressure values in bar
pressures=(1.0e-03 1.0e-02 2.5e-02 5.0e-02 7.5e-02 1.0e-01 2.5e-01 5.0e-01 7.5e-01 1.0e+00)

# Pyrolysis gas non-dimensional flux values
bp_gs=(0.00000e+00 2.00000e-02 4.00000e-02 7.00000e-02 1.00000e-01 1.50000e-01 2.00000e-01 2.50000e-01 3.20000e-01 4.00000e-01 5.00000e-01 6.00000e-01 7.00000e-01 8.00000e-01 1.00000e+00 1.20000e+00 1.50000e+00 1.90000e+00 2.40000e+00 3.00000e+00 4.00000e+00 5.50000e+00 7.50000e+00 1.00000e+01)

# Temperature range and steps
T_min=300
T_max=3500
dT=50

# Check for global output file existence and ask user what to do.
if [ -e $out ]
then
echo "File $out exists! Do you wish to continue and overwrite it (type 1 or 2)?"
    select yn in "Yes" "No"
    do
        case $yn in
            Yes ) echo "Deleting file and continue script execution.";
                rm -rf $out; break;;
            No ) echo "Quitting, script not executed."; exit;;
        esac
    done
```

```
fi

# Loop over pressures
for pressure in "${pressures[@]}"
do
    # Loop over pyrolysis gas flux
    for bp_g in "${bp_gs[@]}"
    do
        if [ $bp_g == ${bp_gs[0]} ] && [ $pressure == ${pressures[0]} ]
        then
            echo "P=$pressure [bar] & B'g=$bp_g" > $out
        else
            echo "P=$pressure [bar] & B'g=$bp_g" >> $out
        fi
# Call bprime and
        bprime $T_min $T_max $dT $pressure $bp_g $mixture BLedge $pyro |
            tee -a out p_${pressure}_Bpg_${bp_g}.dat >/dev/null

        wait
        echo "##########################################################"
            >> out
    done
done
```

E. B' tables for air atmosphere

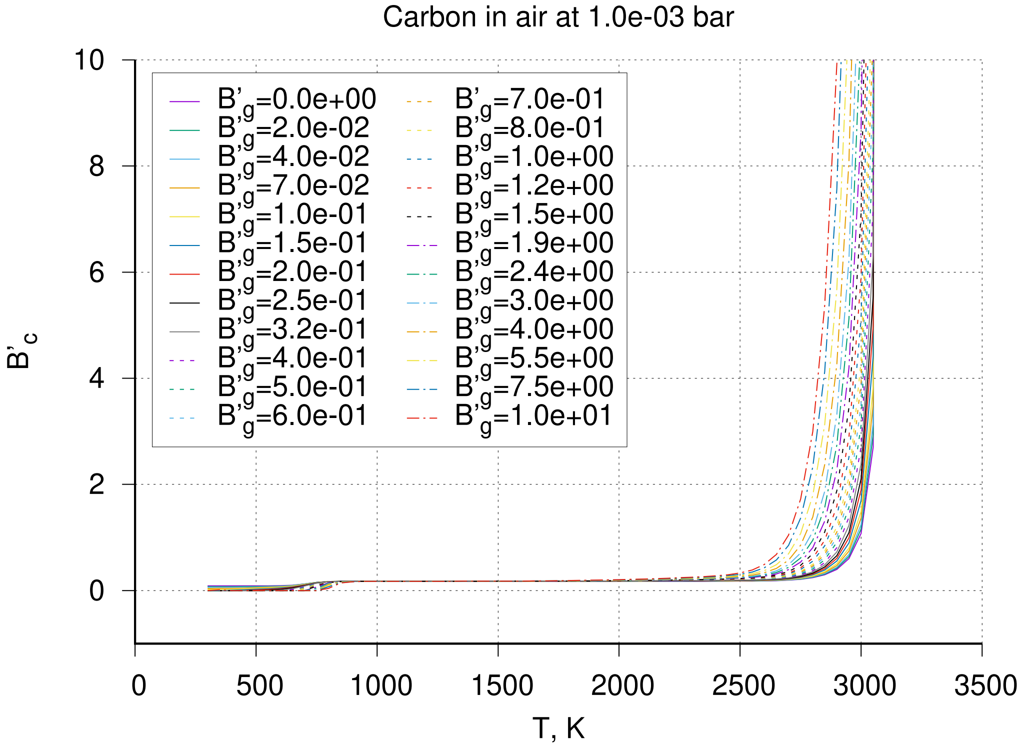

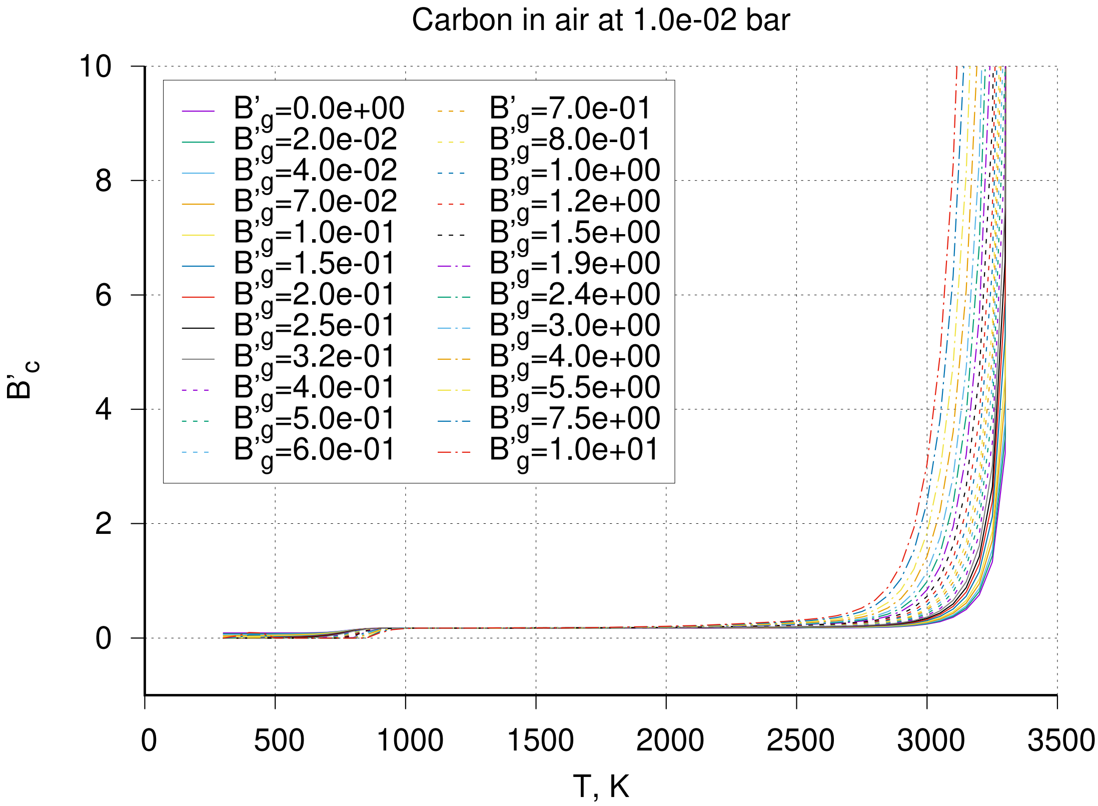
Carbon in air at 1.0e-02 bar
B'c
T, K
B'g=0.0e+00
B'g=2.0e-02
B'g=4.0e-02
B'g=7.0e-02
B'g=1.0e-01
B'g=1.5e-01
B'g=2.0e-01
B'g=2.5e-01
B'g=3.2e-01
B'g=4.0e-01
B'g=5.0e-01
B'g=6.0e-01
B'g=7.0e-01
B'g=8.0e-01
B'g=1.0e+00
B'g=1.2e+00
B'g=1.5e+00
B'g=1.9e+00
B'g=2.4e+00
B'g=3.0e+00
B'g=4.0e+00
B'g=5.5e+00
B'g=7.5e+00
B'g=1.0e+01

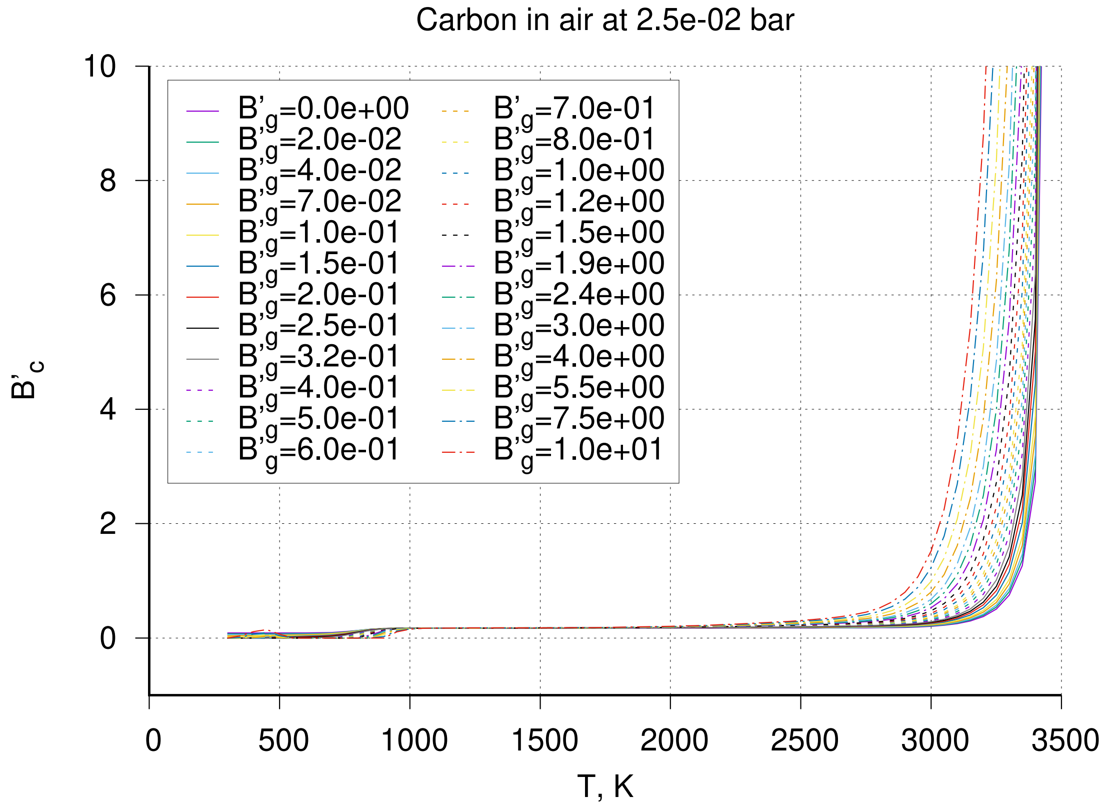
Carbon in air at 2.5e-02 bar
B'c
T, K
0
500
1000
1500
2000
2500
3000
3500
10
8
6
4
2
0
B'g=0.0e+00
B'g=2.0e-02
B'g=4.0e-02
B'g=7.0e-02
B'g=1.0e-01
B'g=1.5e-01
B'g=2.0e-01
B'g=2.5e-01
B'g=3.2e-01
B'g=4.0e-01
B'g=5.0e-01
B'g=6.0e-01
B'g=7.0e-01
B'g=8.0e-01
B'g=1.0e+00
B'g=1.2e+00
B'g=1.5e+00
B'g=1.9e+00
B'g=2.4e+00
B'g=3.0e+00
B'g=4.0e+00
B'g=5.5e+00
B'g=7.5e+00
B'g=1.0e+01

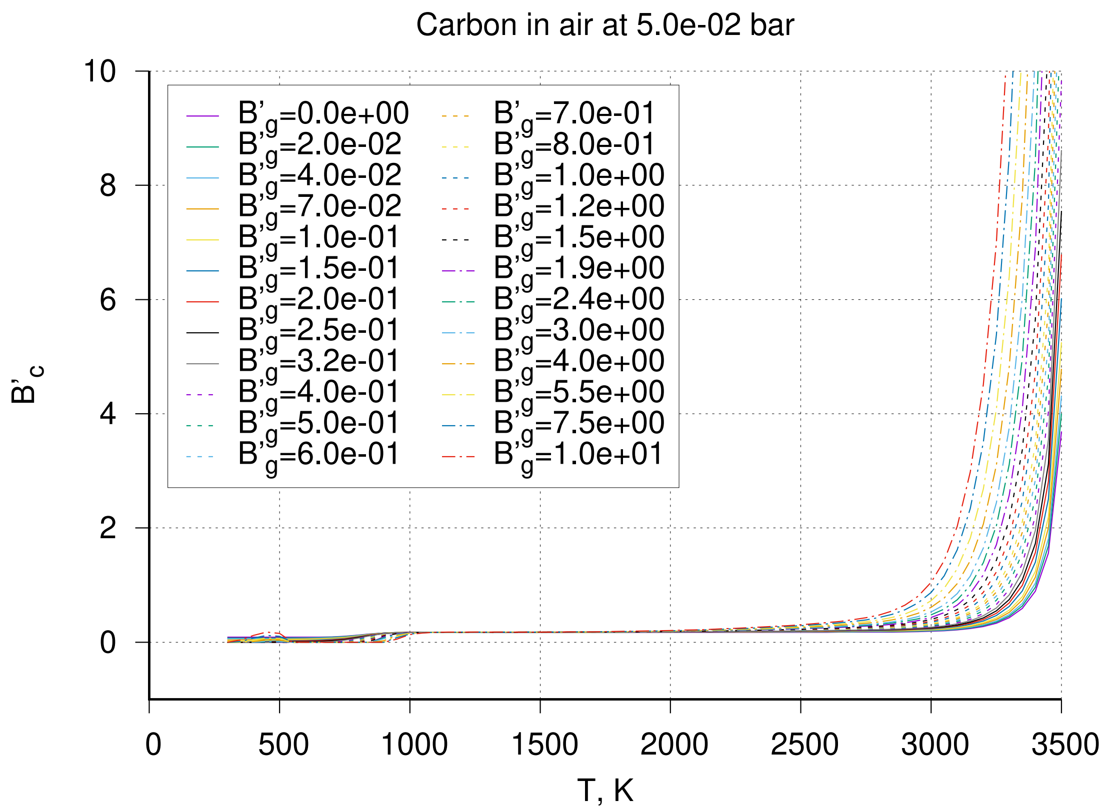
Carbon in air at 5.0e-02 bar
B'g=0.0e+00
B'g=2.0e-02
B'g=4.0e-02
B'g=7.0e-02
B'g=1.0e-01
B'g=1.5e-01
B'g=2.0e-01
B'g=2.5e-01
B'g=3.2e-01
B'g=4.0e-01
B'g=5.0e-01
B'g=6.0e-01
B'g=7.0e-01
B'g=8.0e-01
B'g=1.0e+00
B'g=1.2e+00
B'g=1.5e+00
B'g=1.9e+00
B'g=2.4e+00
B'g=3.0e+00
B'g=4.0e+00
B'g=5.5e+00
B'g=7.5e+00
B'g=1.0e+01
B'c
T, K
0
2
4
6
8
10
0
500
1000
1500
2000
2500
3000
3500

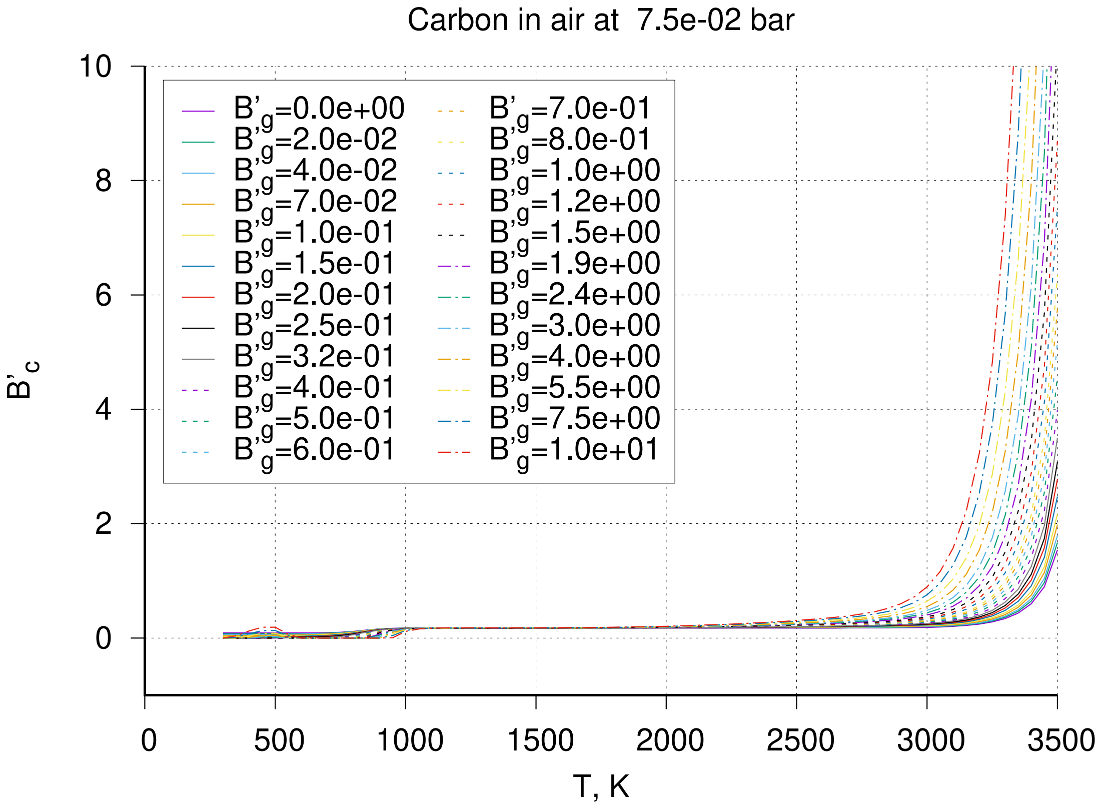
Carbon in air at 7.5e-02 bar
B'c
T, K
B'g=0.0e+00
B'g=2.0e-02
B'g=4.0e-02
B'g=7.0e-02
B'g=1.0e-01
B'g=1.5e-01
B'g=2.0e-01
B'g=2.5e-01
B'g=3.2e-01
B'g=4.0e-01
B'g=5.0e-01
B'g=6.0e-01
B'g=7.0e-01
B'g=8.0e-01
B'g=1.0e+00
B'g=1.2e+00
B'g=1.5e+00
B'g=1.9e+00
B'g=2.4e+00
B'g=3.0e+00
B'g=4.0e+00
B'g=5.5e+00
B'g=7.5e+00
B'g=1.0e+01
0
500
1000
1500
2000
2500
3000
3500
10
8
6
4
2
0

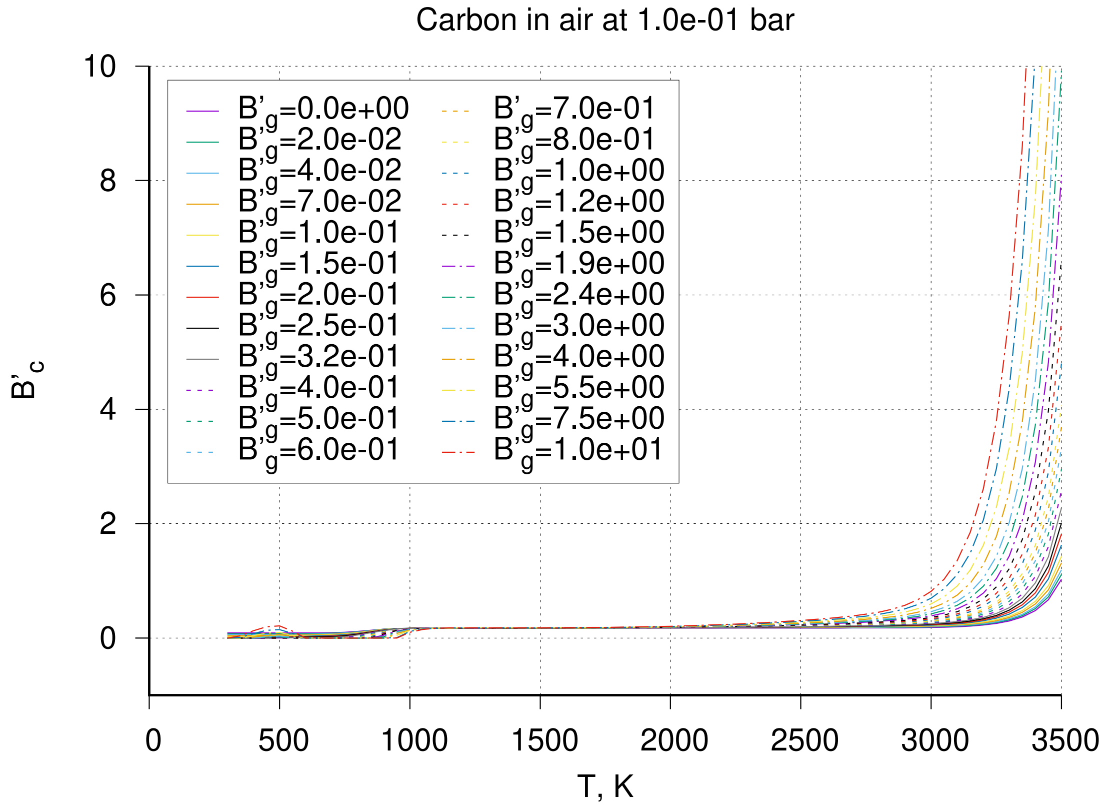
Carbon in air at 1.0e-01 bar
B'c
T, K
0
500
1000
1500
2000
2500
3000
3500
10
8
6
4
2
0
B'g=0.0e+00
B'g=2.0e-02
B'g=4.0e-02
B'g=7.0e-02
B'g=1.0e-01
B'g=1.5e-01
B'g=2.0e-01
B'g=2.5e-01
B'g=3.2e-01
B'g=4.0e-01
B'g=5.0e-01
B'g=6.0e-01
B'g=7.0e-01
B'g=8.0e-01
B'g=1.0e+00
B'g=1.2e+00
B'g=1.5e+00
B'g=1.9e+00
B'g=2.4e+00
B'g=3.0e+00
B'g=4.0e+00
B'g=5.5e+00
B'g=7.5e+00
B'g=1.0e+01

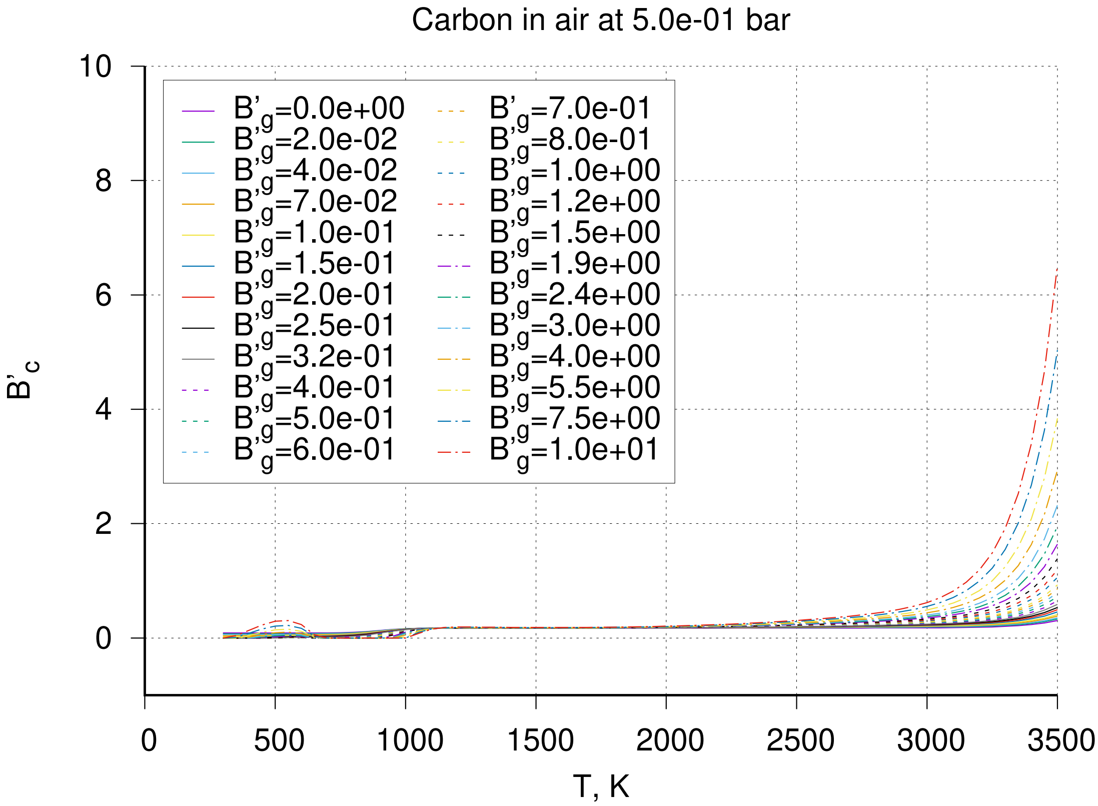
Carbon in air at 5.0e-01 bar
B'c
T, K
0
2
4
6
8
10
0
500
1000
1500
2000
2500
3000
3500
B'g=0.0e+00
B'g=2.0e-02
B'g=4.0e-02
B'g=7.0e-02
B'g=1.0e-01
B'g=1.5e-01
B'g=2.0e-01
B'g=2.5e-01
B'g=3.2e-01
B'g=4.0e-01
B'g=5.0e-01
B'g=6.0e-01
B'g=7.0e-01
B'g=8.0e-01
B'g=1.0e+00
B'g=1.2e+00
B'g=1.5e+00
B'g=1.9e+00
B'g=2.4e+00
B'g=3.0e+00
B'g=4.0e+00
B'g=5.5e+00
B'g=7.5e+00
B'g=1.0e+01

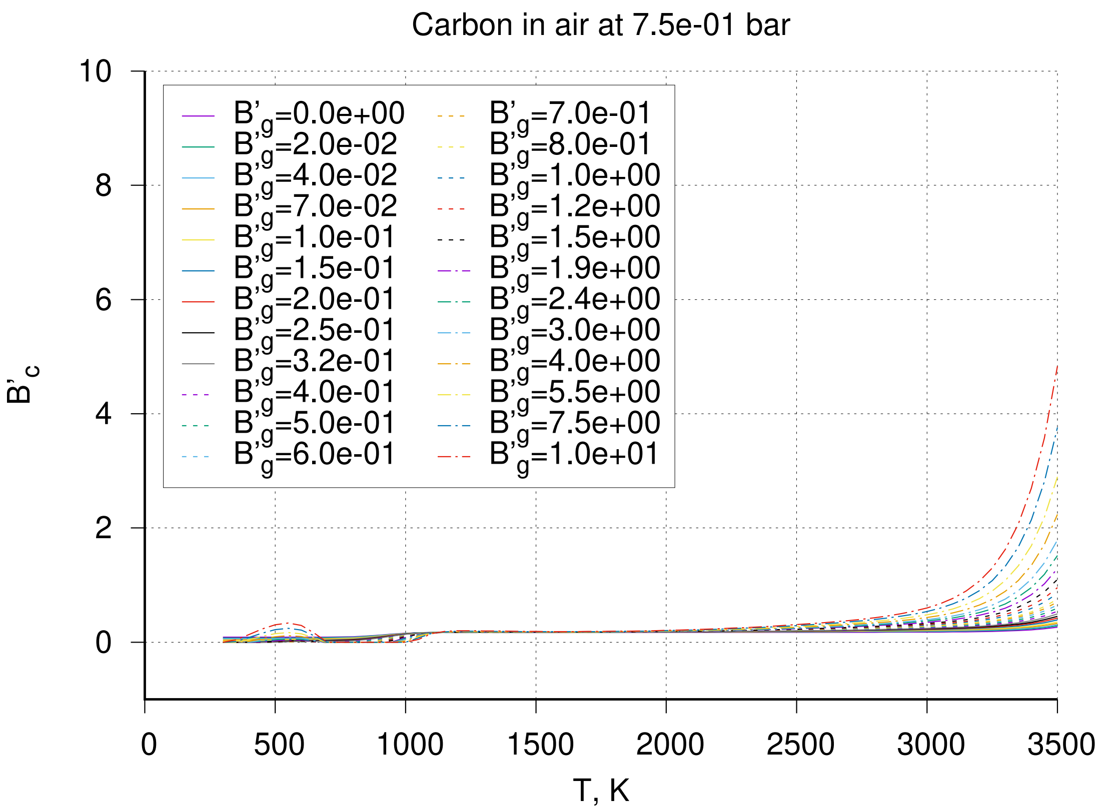
Carbon in air at 7.5e-01 bar
B'g=0.0e+00
B'g=2.0e-02
B'g=4.0e-02
B'g=7.0e-02
B'g=1.0e-01
B'g=1.5e-01
B'g=2.0e-01
B'g=2.5e-01
B'g=3.2e-01
B'g=4.0e-01
B'g=5.0e-01
B'g=6.0e-01
B'g=7.0e-01
B'g=8.0e-01
B'g=1.0e+00
B'g=1.2e+00
B'g=1.5e+00
B'g=1.9e+00
B'g=2.4e+00
B'g=3.0e+00
B'g=4.0e+00
B'g=5.5e+00
B'g=7.5e+00
B'g=1.0e+01
B'c
T, K

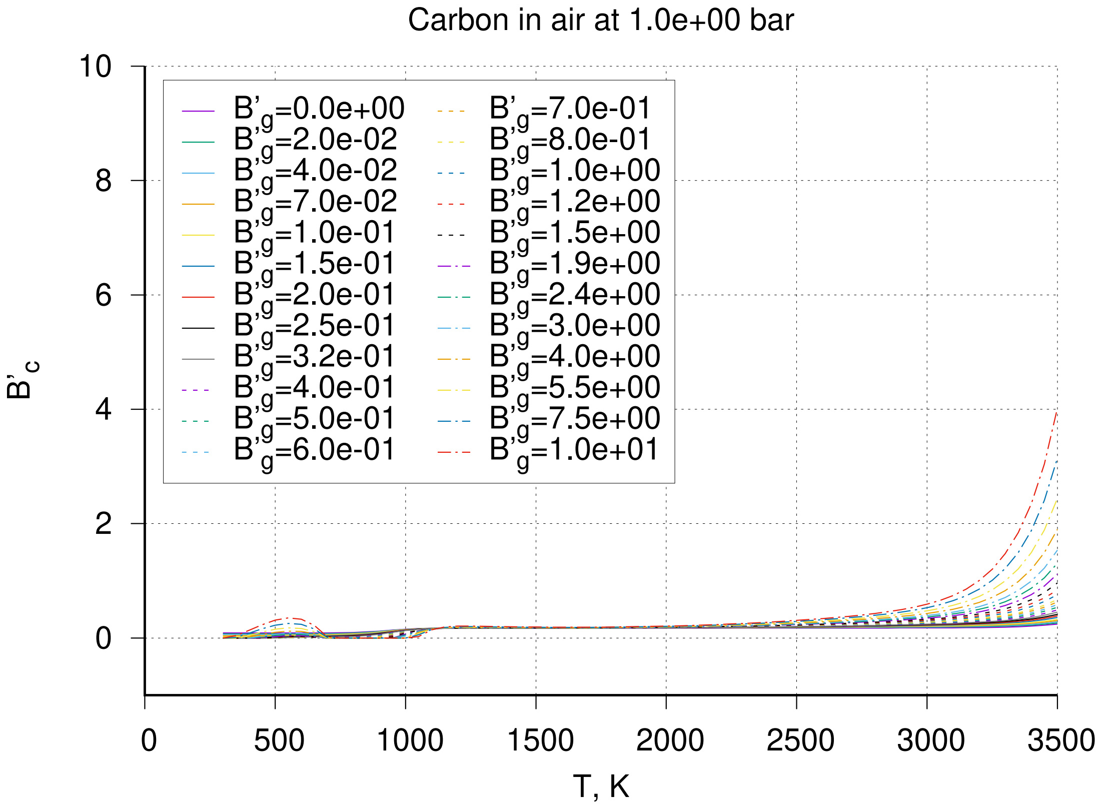
Carbon in air at 1.0e+00 bar
B'c
T, K
B'g=0.0e+00
B'g=2.0e-02
B'g=4.0e-02
B'g=7.0e-02
B'g=1.0e-01
B'g=1.5e-01
B'g=2.0e-01
B'g=2.5e-01
B'g=3.2e-01
B'g=4.0e-01
B'g=5.0e-01
B'g=6.0e-01
B'g=7.0e-01
B'g=8.0e-01
B'g=1.0e+00
B'g=1.2e+00
B'g=1.5e+00
B'g=1.9e+00
B'g=2.4e+00
B'g=3.0e+00
B'g=4.0e+00
B'g=5.5e+00
B'g=7.5e+00
B'g=1.0e+01
10
8
6
4
2
0
0
500
1000
1500
2000
2500
3000
3500

F. B' tables for nitrogen atmosphere

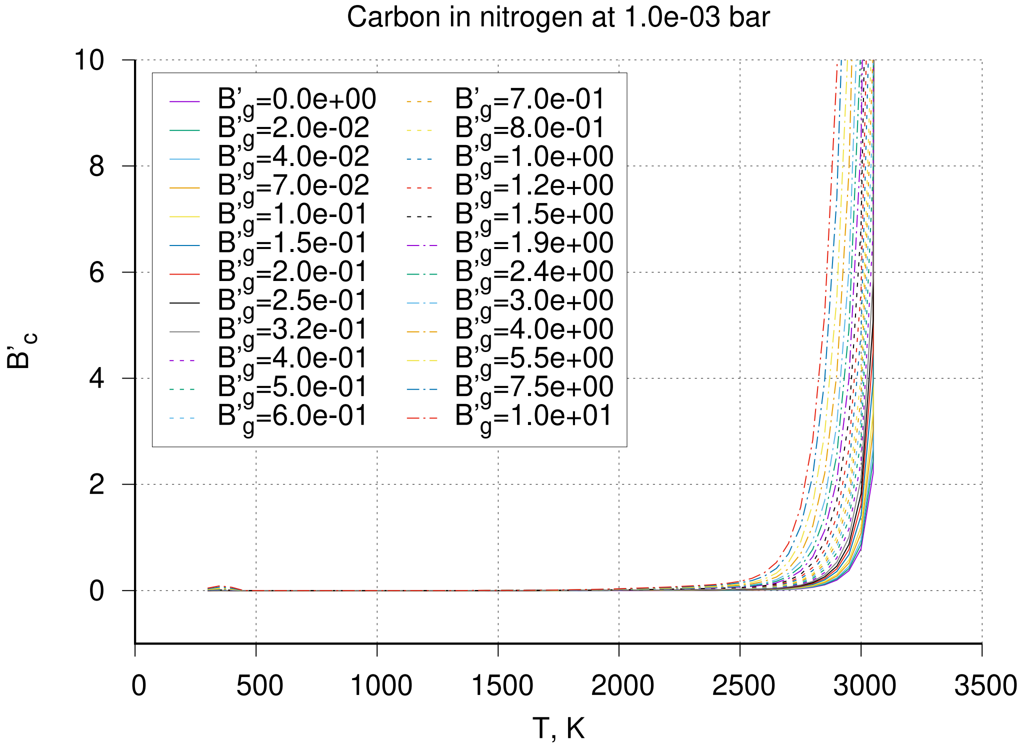

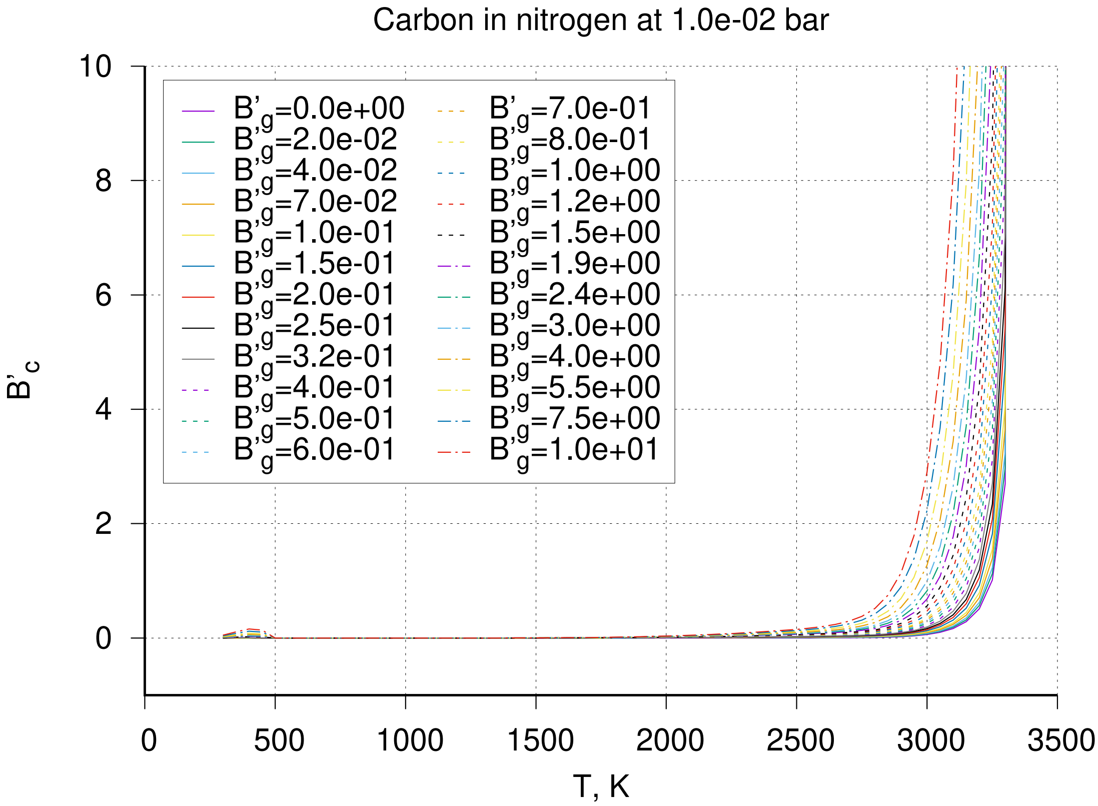
Carbon in nitrogen at 1.0e-02 bar
B'c
T, K
B'g=0.0e+00
B'g=2.0e-02
B'g=4.0e-02
B'g=7.0e-02
B'g=1.0e-01
B'g=1.5e-01
B'g=2.0e-01
B'g=2.5e-01
B'g=3.2e-01
B'g=4.0e-01
B'g=5.0e-01
B'g=6.0e-01
B'g=7.0e-01
B'g=8.0e-01
B'g=1.0e+00
B'g=1.2e+00
B'g=1.5e+00
B'g=1.9e+00
B'g=2.4e+00
B'g=3.0e+00
B'g=4.0e+00
B'g=5.5e+00
B'g=7.5e+00
B'g=1.0e+01
10
8
6
4
2
0
0
500
1000
1500
2000
2500
3000
3500

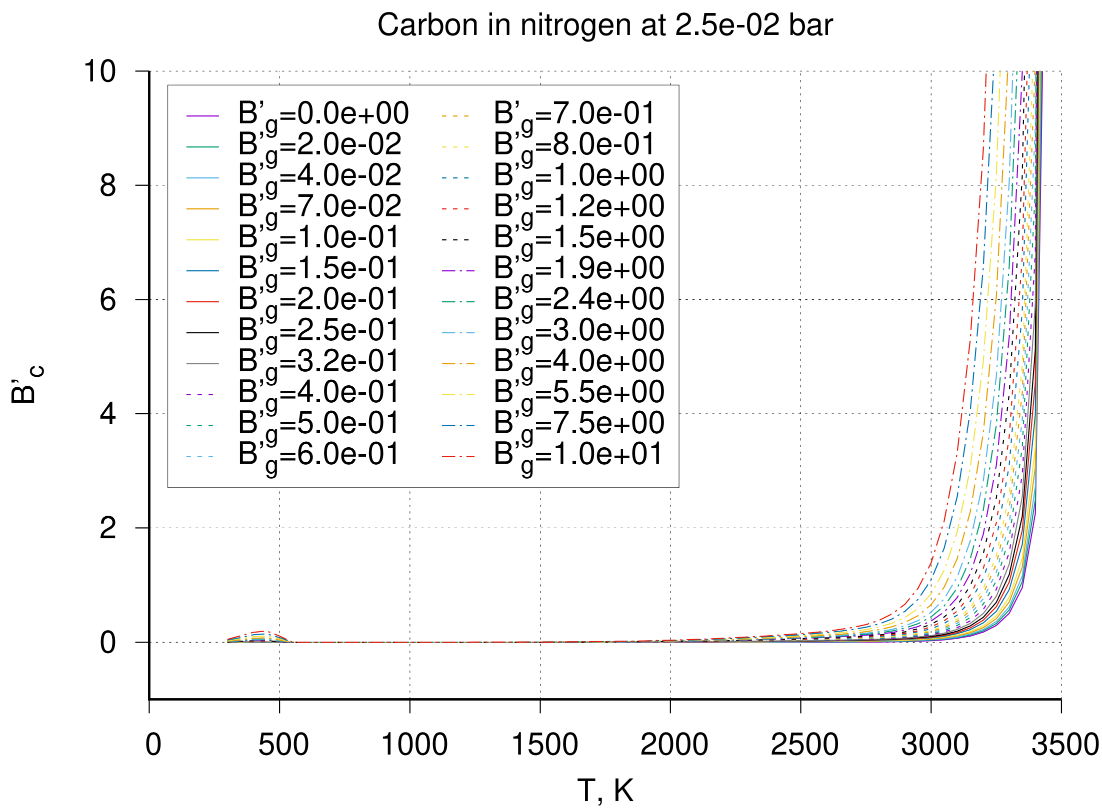
Carbon in nitrogen at 2.5e-02 bar
B'c
T, K
B'g=0.0e+00
B'g=2.0e-02
B'g=4.0e-02
B'g=7.0e-02
B'g=1.0e-01
B'g=1.5e-01
B'g=2.0e-01
B'g=2.5e-01
B'g=3.2e-01
B'g=4.0e-01
B'g=5.0e-01
B'g=6.0e-01
B'g=7.0e-01
B'g=8.0e-01
B'g=1.0e+00
B'g=1.2e+00
B'g=1.5e+00
B'g=1.9e+00
B'g=2.4e+00
B'g=3.0e+00
B'g=4.0e+00
B'g=5.5e+00
B'g=7.5e+00
B'g=1.0e+01
0
2
4
6
8
10
0
500
1000
1500
2000
2500
3000
3500

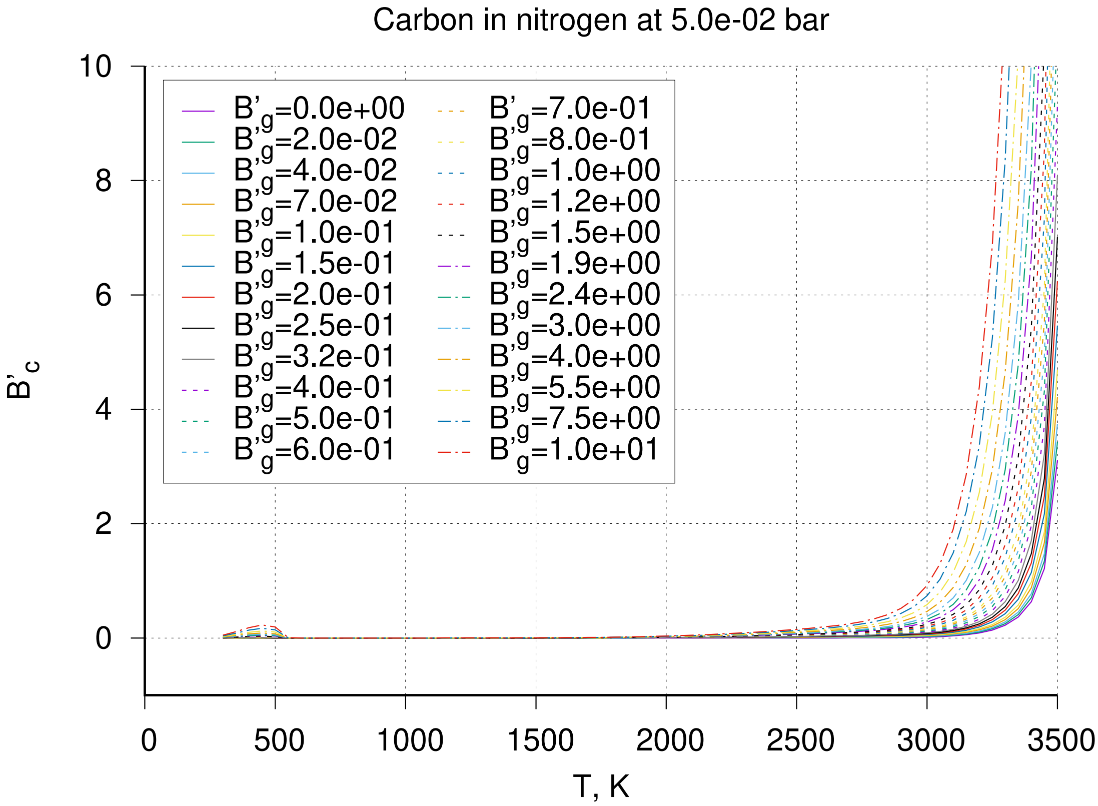
Carbon in nitrogen at 5.0e-02 bar
B'c
T, K
B'g=0.0e+00
B'g=2.0e-02
B'g=4.0e-02
B'g=7.0e-02
B'g=1.0e-01
B'g=1.5e-01
B'g=2.0e-01
B'g=2.5e-01
B'g=3.2e-01
B'g=4.0e-01
B'g=5.0e-01
B'g=6.0e-01
B'g=7.0e-01
B'g=8.0e-01
B'g=1.0e+00
B'g=1.2e+00
B'g=1.5e+00
B'g=1.9e+00
B'g=2.4e+00
B'g=3.0e+00
B'g=4.0e+00
B'g=5.5e+00
B'g=7.5e+00
B'g=1.0e+01

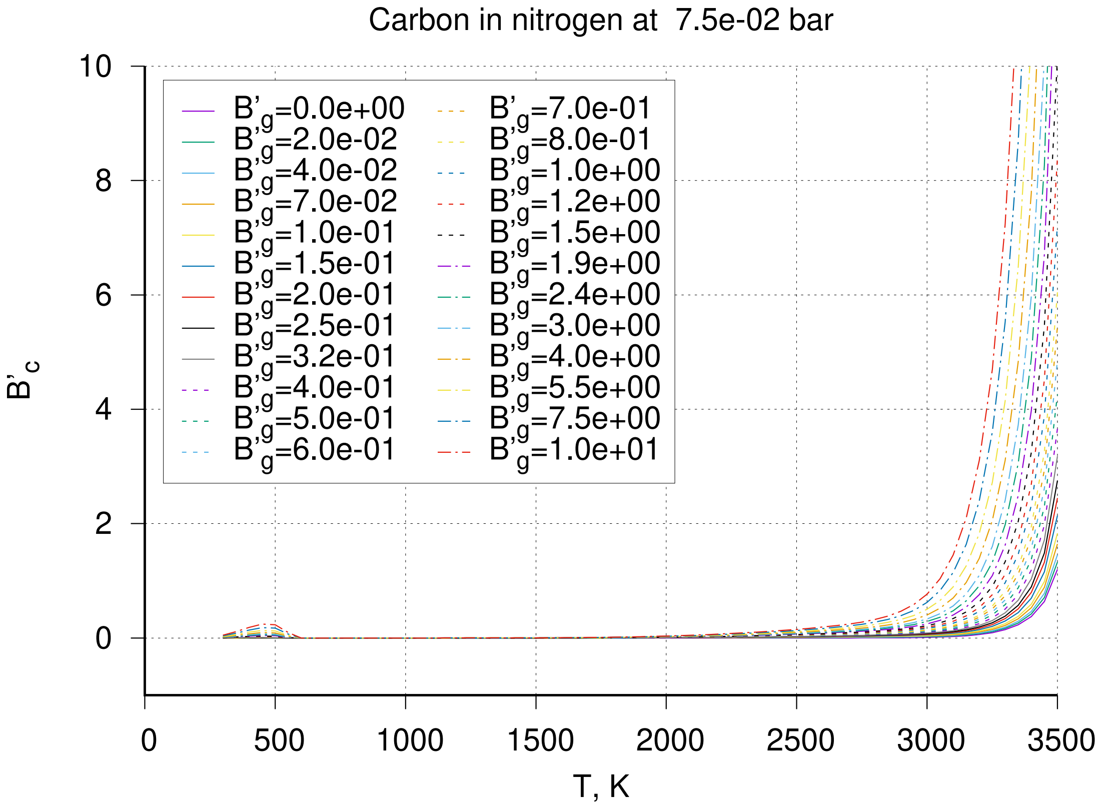
Carbon in nitrogen at 7.5e-02 bar
B'c
T, K
B'g=0.0e+00
B'g=2.0e-02
B'g=4.0e-02
B'g=7.0e-02
B'g=1.0e-01
B'g=1.5e-01
B'g=2.0e-01
B'g=2.5e-01
B'g=3.2e-01
B'g=4.0e-01
B'g=5.0e-01
B'g=6.0e-01
B'g=7.0e-01
B'g=8.0e-01
B'g=1.0e+00
B'g=1.2e+00
B'g=1.5e+00
B'g=1.9e+00
B'g=2.4e+00
B'g=3.0e+00
B'g=4.0e+00
B'g=5.5e+00
B'g=7.5e+00
B'g=1.0e+01

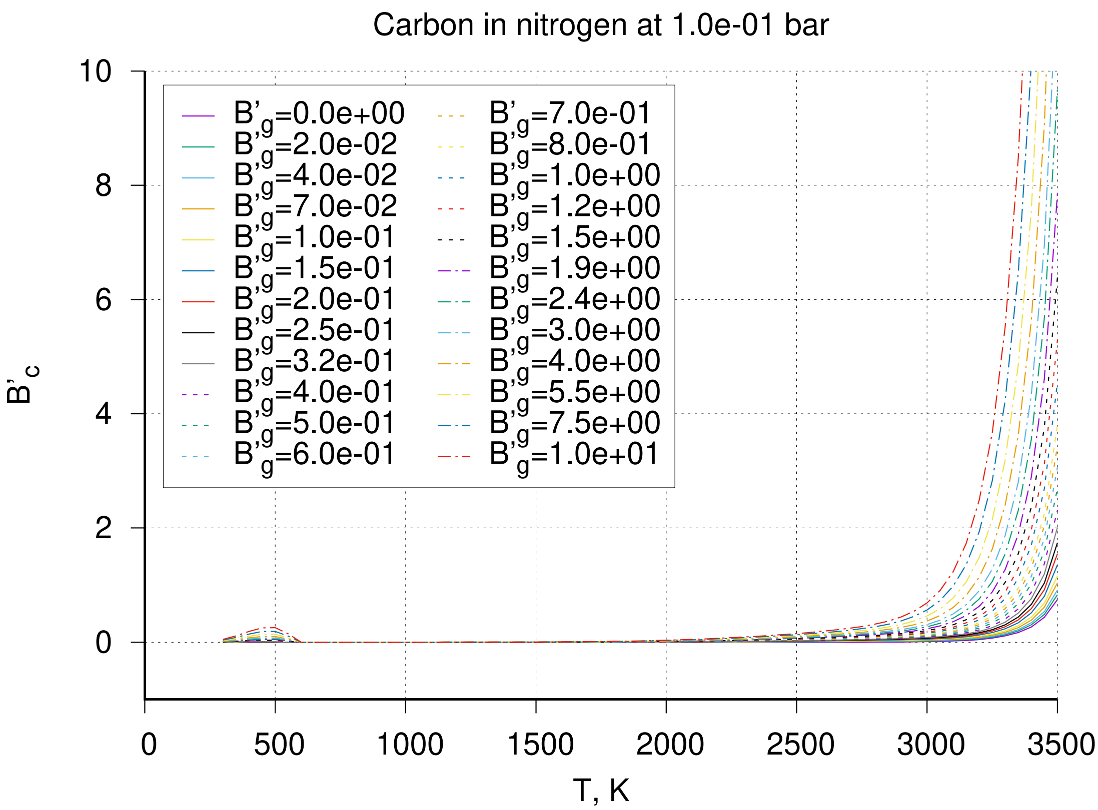
Carbon in nitrogen at 1.0e-01 bar
B'c
T, K
B'g=0.0e+00
B'g=2.0e-02
B'g=4.0e-02
B'g=7.0e-02
B'g=1.0e-01
B'g=1.5e-01
B'g=2.0e-01
B'g=2.5e-01
B'g=3.2e-01
B'g=4.0e-01
B'g=5.0e-01
B'g=6.0e-01
B'g=7.0e-01
B'g=8.0e-01
B'g=1.0e+00
B'g=1.2e+00
B'g=1.5e+00
B'g=1.9e+00
B'g=2.4e+00
B'g=3.0e+00
B'g=4.0e+00
B'g=5.5e+00
B'g=7.5e+00
B'g=1.0e+01
0
2
4
6
8
10
0
500
1000
1500
2000
2500
3000
3500

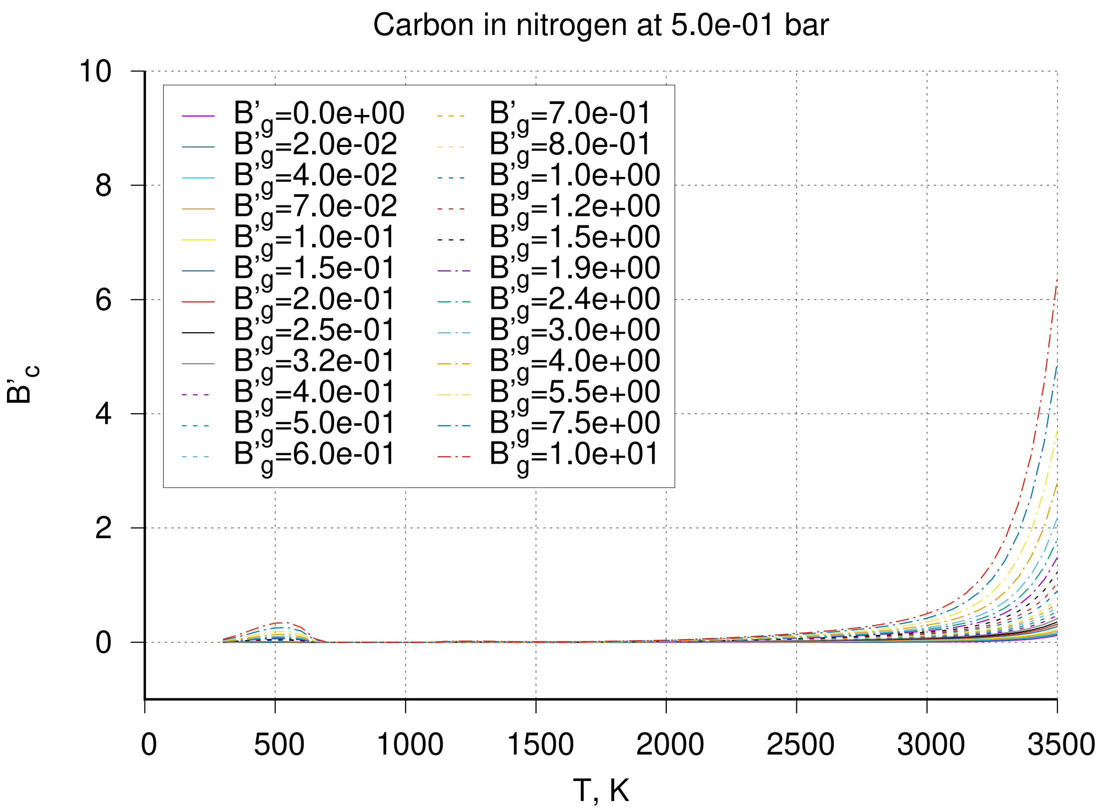
Carbon in nitrogen at 5.0e-01 bar
B'c
T, K
B'g=0.0e+00
B'g=2.0e-02
B'g=4.0e-02
B'g=7.0e-02
B'g=1.0e-01
B'g=1.5e-01
B'g=2.0e-01
B'g=2.5e-01
B'g=3.2e-01
B'g=4.0e-01
B'g=5.0e-01
B'g=6.0e-01
B'g=7.0e-01
B'g=8.0e-01
B'g=1.0e+00
B'g=1.2e+00
B'g=1.5e+00
B'g=1.9e+00
B'g=2.4e+00
B'g=3.0e+00
B'g=4.0e+00
B'g=5.5e+00
B'g=7.5e+00
B'g=1.0e+01
0
2
4
6
8
10
0
500
1000
1500
2000
2500
3000
3500

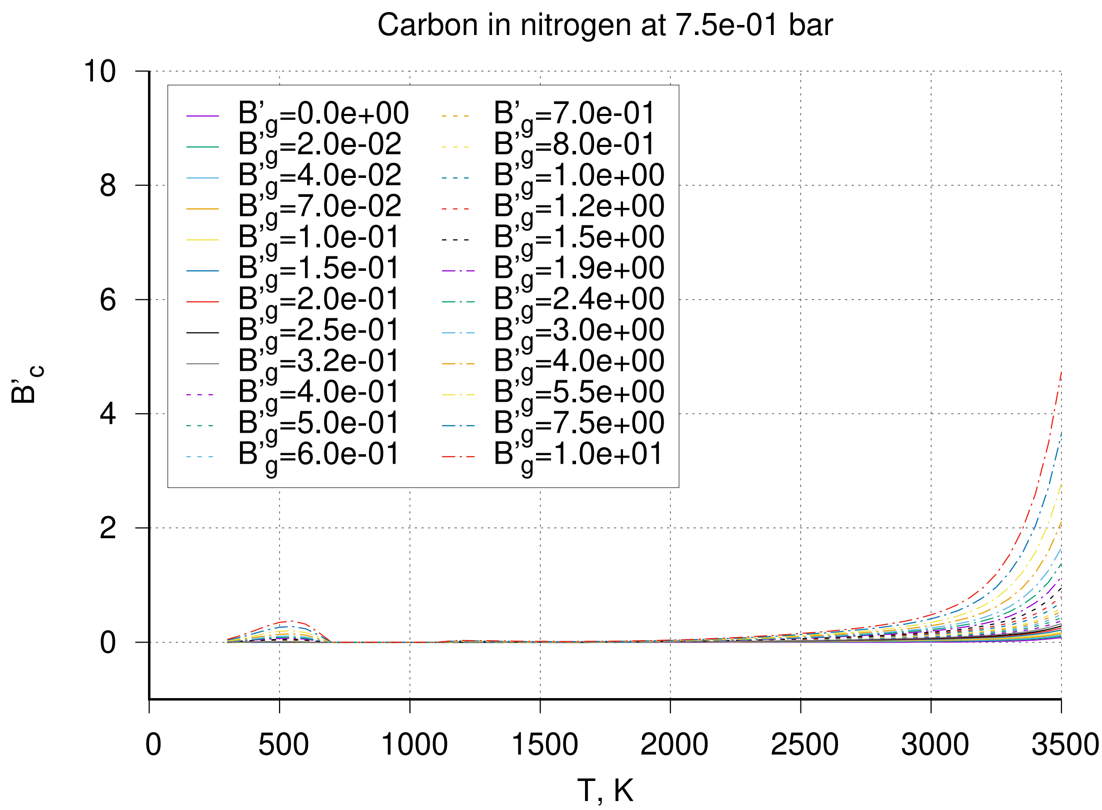
Carbon in nitrogen at 7.5e-01 bar
B'g=0.0e+00
B'g=2.0e-02
B'g=4.0e-02
B'g=7.0e-02
B'g=1.0e-01
B'g=1.5e-01
B'g=2.0e-01
B'g=2.5e-01
B'g=3.2e-01
B'g=4.0e-01
B'g=5.0e-01
B'g=6.0e-01
B'g=7.0e-01
B'g=8.0e-01
B'g=1.0e+00
B'g=1.2e+00
B'g=1.5e+00
B'g=1.9e+00
B'g=2.4e+00
B'g=3.0e+00
B'g=4.0e+00
B'g=5.5e+00
B'g=7.5e+00
B'g=1.0e+01
B'c
T, K
0
2
4
6
8
10
0
500
1000
1500
2000
2500
3000
3500

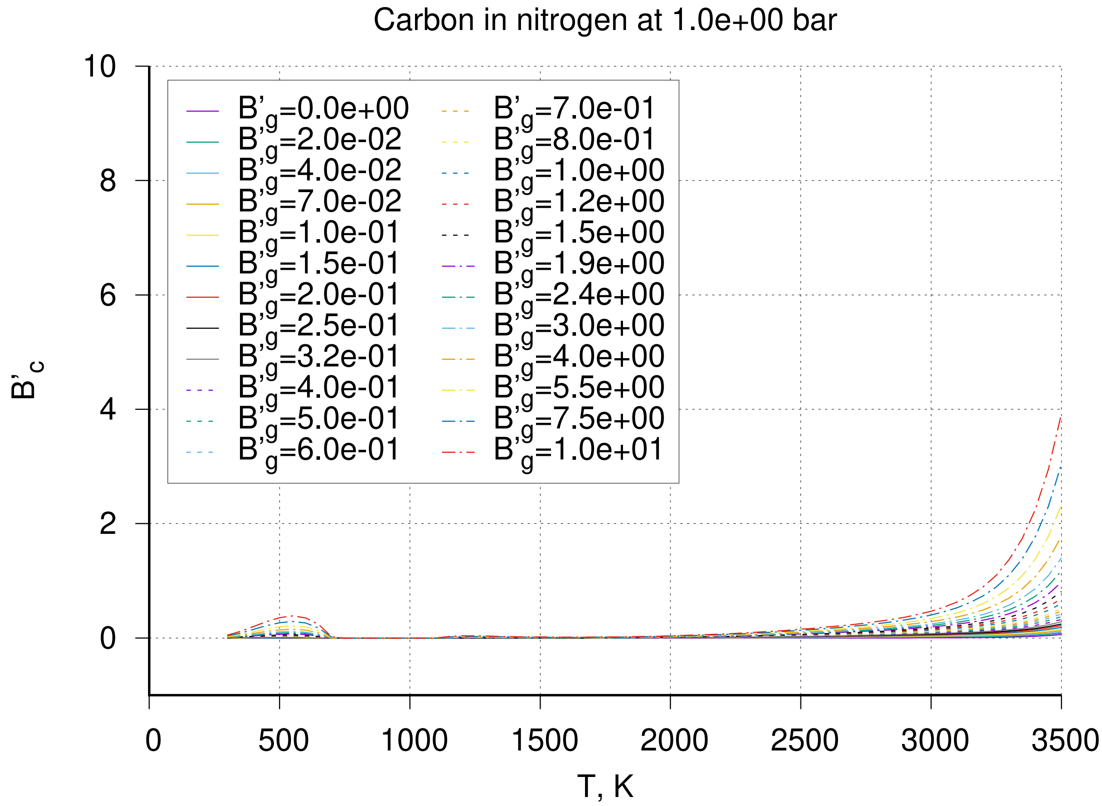
Carbon in nitrogen at 1.0e+00 bar
B'c
T, K
0
500
1000
1500
2000
2500
3000
3500
10
8
6
4
2
0
B'g=0.0e+00
B'g=2.0e-02
B'g=4.0e-02
B'g=7.0e-02
B'g=1.0e-01
B'g=1.5e-01
B'g=2.0e-01
B'g=2.5e-01
B'g=3.2e-01
B'g=4.0e-01
B'g=5.0e-01
B'g=6.0e-01
B'g=7.0e-01
B'g=8.0e-01
B'g=1.0e+00
B'g=1.2e+00
B'g=1.5e+00
B'g=1.9e+00
B'g=2.4e+00
B'g=3.0e+00
B'g=4.0e+00
B'g=5.5e+00
B'g=7.5e+00
B'g=1.0e+01